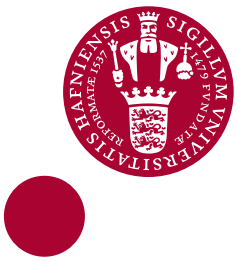

Mapping Cropland Abandonment in the Aral Sea Basin with MODIS Time Series

Löw, Fabian; Prishchepov, Alexander Vladimirovich; Waldner, Francois; Dubovyk, Olena; Akramkhanov, Akmal; Biradar, Chandrashekhar; Lamers, John P. A.

Published in:
Remote Sensing

DOI:
10.3390/rs10020159

Publication date:
2018

Document version
Publisher's PDF, also known as Version of record

remote sensing

MDPI

Article

Mapping Cropland Abandonment in the Aral Sea Basin with MODIS Time Series

Fabian Löw [1,2,*], Alexander V. Prishchepov [3,4,5], François Waldner [6,7], Olena Dubovyk [8], Akmal Akramkhanov [1], Chandrashekhar Biradar [1] and John P. A. Lamers [8]

1 International Centre for Agricultural Research in Dry Areas (ICARDA), 11431 Cairo, Egypt; A.Akramkhanov@cgiar.org (A.A.); C.Biradar@cgiar.org (C.B.)
2 MapTailor Geospatial Consulting, 53113 Bonn, Germany
3 Department of Geosciences and Natural Resource Management (IGN), University of Copenhagen, 1165 København, Denmark; alpr@ign.ku.dk
4 Leibniz Institute of Agricultural Development in Transition Economies (IAMO), 06120 Halle (Saale), Germany
5 Institute of Environmental Sciences, Kazan Federal University, 420008 Kazan, Russia
6 Earth and Life Institute-Environment, Université Catholique de Louvain, 2 Croix du Sud, 1348 Louvain-la-Neuve, Belgium; franz.waldner@csiro.au
7 CSIRO Agriculture & Food, 306 Carmody Road, St Lucia, QLD 4067, Australia
8 Department of Geography, Rheinische-Friedrich-Wilhelms-Universität, 53113 Bonn, Germany; odubovyk@uni-bonn.de (O.D.); jlamers@uni-bonn.de (J.P.A.L.)
* Correspondence: fabian.loew@maptailor.net

Received: 18 November 2017; Accepted: 16 January 2018; Published: 23 January 2018

Abstract: Cropland abandonment is globally widespread and has strong repercussions for regional food security and the environment. Statistics suggest that one of the hotspots of abandoned cropland is located in the drylands of the Aral Sea Basin (ASB), which covers parts of post-Soviet Central Asia, Afghanistan and Iran. To date, the exact spatial and temporal extents of abandoned cropland remain unclear, which hampers land-use planning. Abandoned land is a potentially valuable resource for alternative land uses. Here, we mapped the abandoned cropland in the drylands of the ASB with a time series of the Normalized Difference Vegetation Index (NDVI) from the Moderate Resolution Imaging Spectroradiometer (MODIS) from 2003–2016. To overcome the restricted ability of a single classifier to accurately map land-use classes across large areas and agro-environmental gradients, "stratum-specific" classifiers were calibrated and classification results were fused based on a locally weighted decision fusion approach. Next, the agro-ecological suitability of abandoned cropland areas was evaluated. The stratum-specific classification approach yielded an overall accuracy of 0.879, which was significantly more accurate ($p < 0.05$) than a "global" classification without stratification, which had an accuracy of 0.811. In 2016, the classification results showed that 13% (1.15 Mha) of the observed irrigated cropland in the ASB was idle (abandoned). Cropland abandonment occurred mostly in the Amudarya and Syrdarya downstream regions and was associated with degraded land and areas prone to water stress. Despite the almost twofold population growth and increasing food demand in the ASB area from 1990 to 2016, abandoned cropland was also located in areas with high suitability for farming. The map of abandoned cropland areas provides a novel basis for assessing the causes leading to abandoned cropland in the ASB. This contributes to assessing the suitability of abandoned cropland for food or bioenergy production, carbon storage, or assessing the environmental trade-offs and social constraints of recultivation.

Keywords: abandoned cropland; Aral Sea Basin; change detection; land use; decision fusion; MODIS

1. Introduction

Agricultural production must sustainably increase to meet the growing food demand while preserving ecosystem services and biodiversity [1,2]. Given the (global) limits of cropland expansion, approximately 80% of this increase must come from intensification such as the expansion of irrigated crop production [3–5], which already contributes to approximately 44% of global crop production [1].

One of the regions where agricultural lands are scarce is the transboundary Aral Sea Basin (ASB), which covers parts of post-Soviet Central Asia (Uzbekistan, Kazakhstan, Kyrgyzstan, Tajikistan and Turkmenistan), Afghanistan and Iran. This region experienced precipitous population growth in the mentioned countries, increasing from 61 million people in 1990 to 104 million by 2016; the rural population is strongly dependent on the domestic agricultural production [6]. Despite increasing food demand, official statistics and exemplary case studies with satellite imagery suggest that agricultural land abandonment is common in this region and most likely occurs on degraded, irrigated agricultural lands [7–10]. Due to economic restructuring, agricultural land abandonment primarily occurs in the downstream Amudarya and Syrdarya River basins resembling Soviet land-use legacies. Additionally, large tracts of cropland in Afghanistan that partly belong to the ASB were left fallow, for reasons including conflicts and war [11]. Currently, the looming scarcity of water resources and ongoing land degradation [12,13] may further enhance abandonment, causing adverse socio-economic consequences, including reduced income or increased food insecurity [14,15].

A better understanding of the spatial and temporal patterns of abandonment and idle land production potential is important to better assess the drivers of land-use change for developing plausible land-use policies [16–18] and assess the impacts on the carbon cycle [19] as well as the trade-offs between the recultivation or the provision of ecosystem services [20]. A revitalization of currently abandoned land could become particularly plausible in areas where significant investments were made during the Soviet era to establish an irrigation and drainage infrastructure [21,22]. The potential for recultivation depends, however, on the biophysical properties of soils and the land suitability itself [23,24].

The main problem is that agricultural statistics for the ASB are often outdated or of doubtful quality and little knowledge exists about the spatial extent of agricultural land abandonment in the ASB. Remote sensing is a well-known alternative to assess large-scale land-use change. Much progress has been made in mapping land-use/land-cover changes (LULCCs) in drylands using geographic information systems (GIS) and remote sensing, such as with 30-m multiannual imagery from Landsat [25,26], high-resolution RapidEye or Sentinel [7,27,28] and 250-m Moderate Resolution Imaging Spectroradiometer (MODIS) data [29,30]. MODIS data fit well for assessing and mapping LULCC and crop types [31] or land abandonment over large regions in a regular manner [32–35]. Additionally, since fallow periods can be part of the typical crop rotation cycle, it is important to assess several consecutive years to determine whether a field has effectively been abandoned or if it is awaiting future use [7]. Using regular, consecutive image time series such as those provided by MODIS helps avoid misclassification of temporarily fallow-crop rotation [7,29].

Machine-learning classifiers were found to be particularly useful to overcome the complexity related to the accurate separation of spectrally similar classes, such as abandoned cropland and cultivated cropland in drylands [36], particularly at the early stages of abandonment [7,29,33,37]. Vegetation recovery on abandoned irrigated fields in the drylands of the ASB generally follows a certain pathway. It starts with the recovery of annual and multiyear herbaceous species [8,38,39] and gradually, perennial woody species such as shrubs (e.g., black saxaul) and some trees [7] can establish. Depending on time and hydrological and soil properties, bare areas without any vegetation change could also be observed [8,24]. Abandoned, formerly irrigated cropland in drylands may therefore represent a set of multimodal distributions of reflectance for different wavelengths recorded with optical satellite imagery. A previous study pointed to the need to have various input data sets and non-parametric machine learning algorithms to map abandoned cropland [29].

To date, LULCC approaches have relied primarily on single classification methods; thus, low accuracies were often found for LULCC in drylands [36] due to difficulties in mapping spectrally complex classes across large areas with different agro-environmental settings [40]. The physiography and type of plant succession in abandoned areas pose challenges to accurately mapping abandoned cropland across large territories over time [7,29,30]. Cropland abandonment can also be associated with both negative (degradation of vegetation) and positive (vegetation recovery) vegetation trends [41,42]. Thus, despite the general suitability of "global" methods for land cover mapping [43,44], they have less accurate performances than locally calibrated models for land cover mapping [45–48] and capturing accurately all diverging trajectories of land-cover change. Similarly, crop rotation practices may differ from country to country, reflecting different land-use policies, regional food security programs and market conditions. It may pose an additional challenge in the generalization of spectral features for a single classification across a large area [36]. At the same time, a fusion of machine-learning classifiers based on strata (e.g., soil types, landforms, administrative boundaries and further stratum-specific classifiers) may boost classification accuracy, particularly where one classifier is not able to accurately separate classes [36]. However, maps created with different classification methods but with similar accuracies may yield spatial disagreement of classified patterns, i.e., errors are rarely equally distributed in a map [49–51]. Thus, a major challenge for mapping large-scale, abandoned cropland is to achieve spatial continuity and consistency in the final map.

The overarching objective of this study was to develop a method that can map the various trajectories (spectral signatures) of cropland abandonment and to create the first map of cropland abandonment across the ASB. Specifically, we (i) tested whether a decision fusion yielded a statistically significant difference ($p < 0.05$) compared to single classification methods, (ii) allocated the hotspots of abandoned cropland and stable cultivated croplands and (iii) related the patterns of abandoned cropland to crop suitability. To achieve our goals, we combined the principle of random feature selection with stratified classifiers in a novel fashion to create a spatially consistent map of cropland abandonment in the ASB. We stratified the study region based on the administrative boundaries and stratum-specific classifiers were calibrated to map abandoned cropland during the 2003–2016 period based on MODIS Normalized Difference Vegetation Index (NDVI) time series.

2. Materials and Methods

2.1. Study Area

The study area covered the agricultural areas of the ASB, a vast transboundary river basin at the heart of the Eurasian continent [52]. It spreads over 1.76 million km^2 and encompasses the southern part of Kazakhstan, Turkmenistan, Uzbekistan, Kyrgyzstan, Tajikistan and small parts of Afghanistan and Iran in the Tedzhen/Murghab Basin. All of these countries, except Afghanistan and Iran, were once part of the former Soviet Union (Central Asia) [53]. The climate in the irrigated regions of the ASB is mostly dry-arid continental with 100–250 mm of precipitation per year, which mainly falls during the winter (December-February). Precipitation in the mountains can exceed 1,000 mm. Because of the aridity, agriculture in the study area is fully dependent on a dense irrigation and drainage network [13], which was extensively developed during the Soviet era [54]. Therefore, agricultural land is predominantly located downstream of the Amudarya and Syrdarya Rivers. More than half the mean annual runoff in the ASB, which is approximately 114 km^3, is generated in Tajikistan and almost one-quarter is generated in Kyrgyzstan [52]. A large share of the fresh water in these rivers is fed into irrigation systems of ~8.1–8.5 Mha of cropland [55,56]. Today, irrigated production is dominated by cotton and wheat production [57] in areas such as in Turkmenistan [58] and Uzbekistan [59]. Rice is an important crop in areas such as south Kazakhstan [7,60]. The average field sizes throughout the ASB range from 2.19 ha (Karakalpakstan) to 6.74 ha (Fergana) [40].

The post-Soviet countries within the ASB have undergone large transitions in their economy and agricultural production after independence in 1991 (Table 1). During the Soviet era, the typical

crop rotation in Uzbekistan, for instance, was three years of alfalfa followed by six years or more of cotton. The crop rotation changed after the independence in 1991; the share of alfalfa and especially cotton decreased in favor of winter wheat [61,62]. In southern Kazakhstan, the official recommendations [38,61,63,64] may vary following the soil quality [59,65]. However, in southern Kazakhstan, rice and alfalfa form a distinct rotation pattern, which differs from Uzbekistan: after two years of rice cultivation, fields are temporarily set aside from crop production (mainly rice) and alfalfa or other legumes are cultivated for up to three consecutive years for soil regeneration (Table 2). Official statistics indicated a gradual decline of land use in irrigated fields but also a decrease of irrigation intensity in the remaining cultivated fields [10].

2.2. Definition of Cropland Abandonment

Abandoned cropland is defined here as "cropland permanently without management," i.e., land that has not been used (sown but not cropped) for a period longer than the fallow periods practiced under the typical crop rotations in the region (Table 2, usually four or more years). After the succession of agricultural production, shrubs and grasses encroached on abandoned fields—or fields remained bare and devoid of vegetation due to salinization (Figure 1). Due to a water shortage (e.g., droughts) or farmers' decisions, intermitted fallow periods may be longer than under the current management practices [26] but such fields do not necessarily meet the given definition of abandoned. Abandoned fields are characterized by a typical and recognizable vegetation succession, starting with the recovery of annual and multiyear herbaceous species [8,38,39], perennial woody species such as shrubs (e.g., black saxaul) and some trees [7]. When classifying a few consecutive years, previous studies have demonstrated that intermittent fallow periods, e.g., as part of agricultural management, or areas left fallow due to water shortage, can obscure land-use trajectories of abandoned fields that in turn lead to misclassifications [7,29,30].

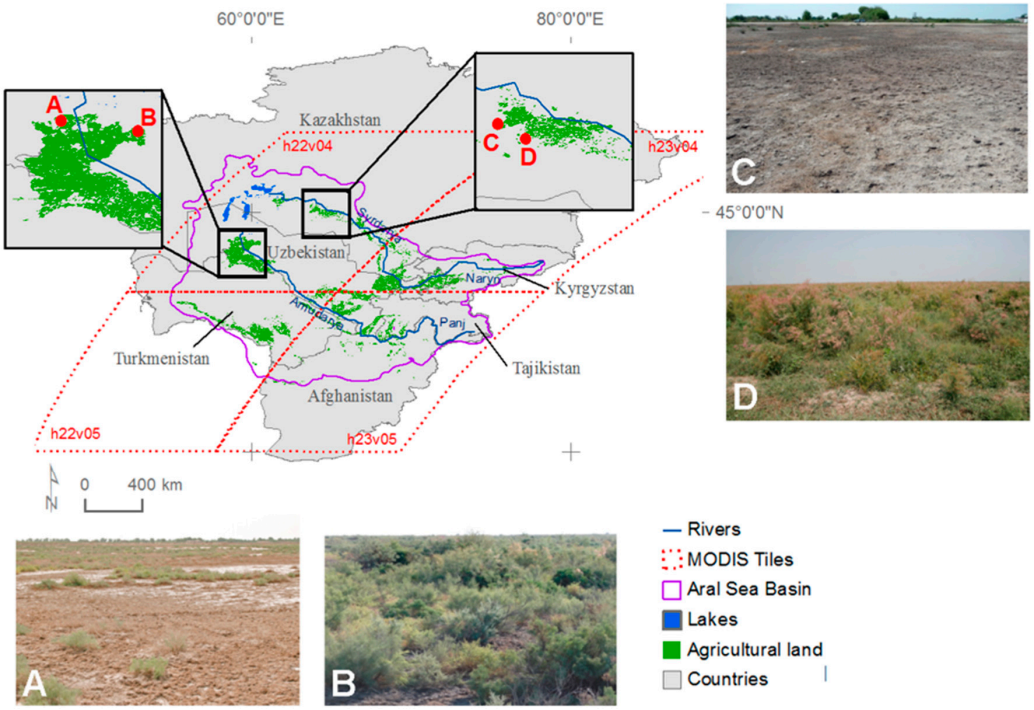

Figure 1. Drylands in the Aral Sea Basin and its irrigated agricultural land. The photographs from 2011 highlight examples of abandoned fields: open (**A**) and dense (**B**) shrubland in Karakalpakstan, bare soil (**C**) and dense shrubland mixed with herbaceous vegetation (**D**) in Kyzyl-Orda, Kazakhstan.

Table 1. Summary of the transition approaches across the post-Soviet countries within the Aral Sea Basin.

Country	Potential Private Ownership after 1990 *	Privatization Strategy *	Allocation Strategy *	Legal Attitude to Transferability after 1990 *	Relevant Legislation *	Agriculture, Value Added (% GDP) in 2014 **	Share of Rural Population in 2014 **
Kazakhstan	Household plots only	None	Shares	Use rights	Presidential Decree on Land Reform, Feb. 1994	4.7	47
Kyrgyzstan	All land	Distribution/conversion	Shares	Moratorium	Presidential Decree on Deepening Land and Agrarian Reform, Feb. 1994 Referendum, June 1998; Presidential Decree on Private Land Ownership, Oct. 1998	17.1	67
Tajikistan	None	None	Shares	Use rights	Land code, Dec. 1996; amended 1999	27.2	73
Turkmenistan	All land	None; virgin land to farmers	Leasehold	None	Constitution, May 1992	No data	50
Uzbekistan	None	None	Leasehold	None	None	18.8	64
Afghanistan	Complex pattern of land management and tenure, shaped by conflict					23.5	74

Note: * Adapted with permission from [66]. ** World Bank.

Table 2. Typical crop rotations for selected areas in the Aral Sea Basin. (Shown is one complete cycle of either the recommended or the mandatory cropping scheme).

Province	Year-1	Year-2	Year-3	Year-4	Year-5	Year-6	Year-7	Year-8	Source
Kazakhstan									
Kazalinsk	Rice	Rice	Fallow	Rice	Rice	Alfalfa	Alfalfa	Alfalfa	[63]
Kyzyl-Orda	Rice	Rice	Alfalfa	Alfalfa	Alfalfa				[60]
Uzbekistan									
Country wide	Cotton *	Cotton *	Cotton	Wheat **	Wheat **				[61,64]
Karakalpakstan ***	Wheat/Alfalfa	Alfalfa	Alfalfa	Cotton	Cotton	Cotton	Cotton		[38]
* 2–3 years of cotton are recommended									[61,64]
** 1–2 years of wheat are recommended, instead of wheat also summer crops such as mung bean, soybean, maize, sunflower or vegetables are cultivated									[38]
*** Expert recommendation for Karakalpakstan; instead of cotton also rice could be cultivated									[38]

2.3. Satellite Data and Preprocessing

Time series of the NDVI from the Terra and Aqua MODIS 250-m instruments were downloaded (16-day L3 Global Collection V006, MOD13Q1 and MYD13Q1) from 2003 to 2016 [67]. Each MODIS tile provides wide spatial coverage (2330 km), a dense frequency of observations and a long-term archive [8,29]. Four 2330 km × 2330 km MODIS tiles (h22v04, h23v04, h22v05 and h23v05) were necessary to cover the study area (Figure 1). Overall, 46 images from both the Terra and Aqua platforms were available for each year and stacked into 14 annual time series.

Several preprocessing steps reduced the effects of residual clouds and shadows, dust, aerosols, off-nadir viewing or low sun zenith angles. First, we excluded pixels flagged as no data and excluded snow/ice or clouds in the MOD13Q1 pixel reliability layer prior to filtering based on MODIS quality assurance information. Only pixels labeled "good data" or "marginal data" were retained. Second, the NDVI time series were smoothed using the Savitzky-Golay approach [68].

Since a gain of classification accuracy was observed when combining phenological metrics with raw time-series data [29,69], several metrics were computed with TIMESAT and served as predictor variables for the following classifications (Figure 2): (a) a median NDVI value of the growing season, (b) 25% and 75% quartiles of the NDVI values of the growing season, (c) the amplitude of the growing season between maximum and minimum NDVI, (d) the standard deviation of NDVI over the growing season and (e) the area under the curve (AUC) from the start to the end of the season (Figure 2). The growing season was defined as starting on Julian day 91 (April 1st, or March 31st on leap years) and ending on Julian day 304 (October 31st, or October 30th in leap years) based on the initial results from TIMESAT [68].

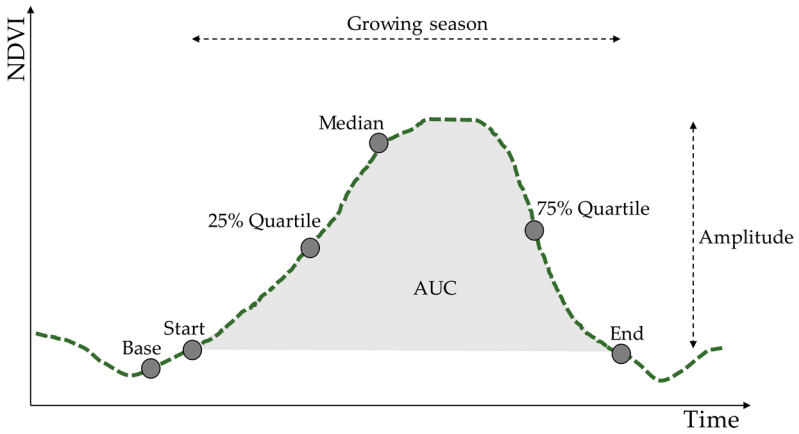

Figure 2. The normalized difference vegetation index (NDVI) phenological metrics for the entire growing season. The phenological metrics are statistical descriptors of the NDVI trajectory of a pixel.

2.4. Training and Testing Data

Reference pixels for algorithm training (calibration) and testing (accuracy assessment) were randomly selected across the study area (Figure 3). In Google Earth^{TM}, high-resolution images from 2016 clearly showed typical indicators of land abandonment, such as advanced shrub encroachment, which supported the labeling process (Figure 4).

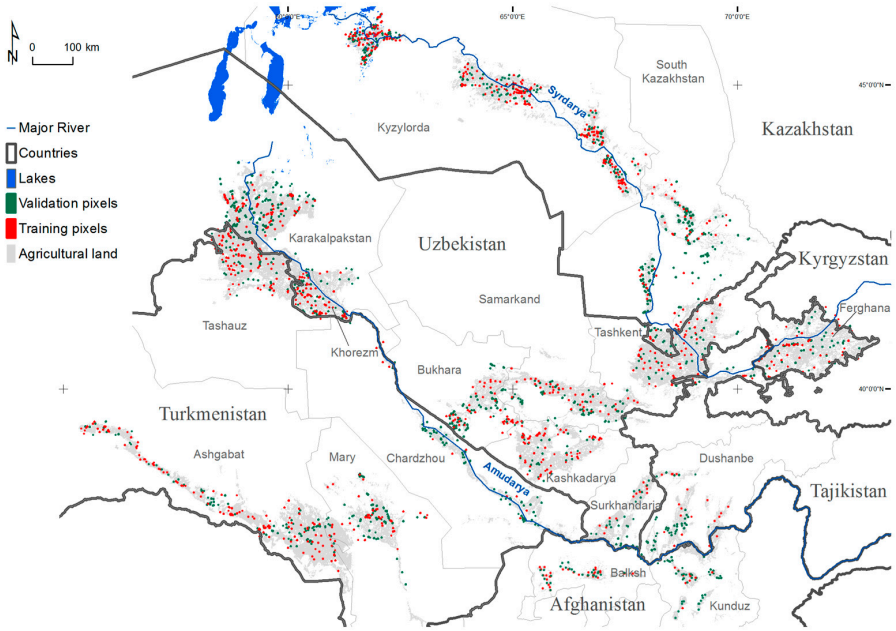

Figure 3. Location of training (red) and validation (green) pixels for determining abandoned vs. active cropland.

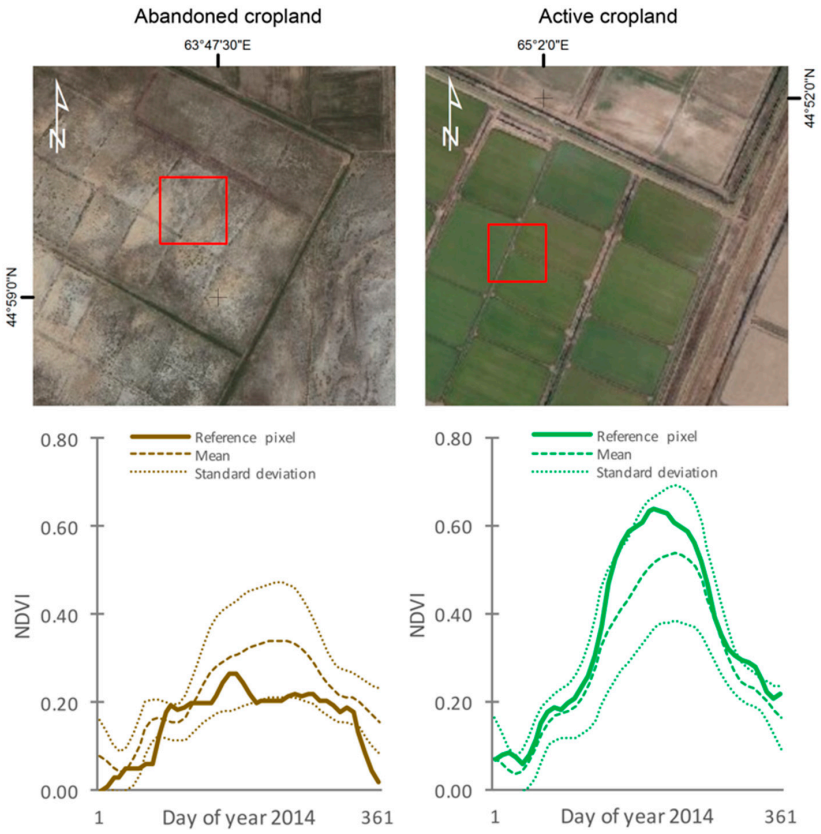

Figure 4. Abandoned (**left**) and active cropland (**right**) MODIS pixels (red squares). The graphs show the mean normalized difference vegetation index (NDVI) of all active and abandoned reference pixels (dashed signatures) and standard deviations (dotted lines). Bold lines represent the NDVI signatures of the two selected reference pixels (Source: Google Earth™ 2016).

To assign the classes for the selected MODIS pixels, we used the following steps. First, for several regions (Karakalpakstan, Kyzyl-Orda and Fergana), non-differential GPS ground data of abandoned fields were available for different years (2008, 2009 and 2014) [7,8,70–72]. This information was used jointly with high-resolution images available via Google Earth™ and MODIS NDVI time-series profiles to assist in the assignment of classes for training data. Phenological signatures of abandoned fields were characterized by smoother, bell-shaped, temporal NDVI signatures, with NDVI values generally below 0.2–0.3 due to low biomass production for semi-natural succession vegetation in drylands [7]. In contrast, active cropland resulted in NDVI temporal profiles with substantially smaller growing season NDVI integrals and a higher NDVI value during the peak of vegetation growth than those of abandoned plots (Figure 2) [73]. Using Google Earth™ to create and validate maps of abandonment and other land cover was also reported in other studies [29,30,35,74,75].

Only pixels with a single dominant land-cover class of at least 85% abundance in the Google Earth™ imagery from 2016 (active or abandoned irrigated cropland) were retained. A buffer of half a MODIS pixel was considered to account for the possible effects of the MODIS large-point spread function [76,77]. To reduce the spatial autocorrelation, a minimum distance of 1.5 km between pixels was ensured.

In total, 7960 reference samples (pixels) of "abandoned vs. active cropland" were randomly selected, with approx. 50% for each class. Approximately one-half of the reference pixels was randomly split and used for the accuracy assessment (4030), while the other half (3930) was used as training data to calibrate/classify active and abandoned cropland.

2.5. Ancillary Data

An existing cropland map for the study area [71] was used to mask out areas where cropland abandonment did not occur (e.g., unmanaged, natural land cover). The map depicts the cropland extent of the region of interest for the period before 2004, which coincided with the onset of the analysis [71]. The overall accuracy of the cropland map, measured with an independent, random sample of 5185 cropland vs. non-cropland test pixels, was 89.8%, whereas the producer's accuracy and user's accuracy for the class "cropland" were 92.1% and 88.2%, respectively. The producer's accuracy and user's accuracy for the class "non-cropland" were 87.5% and 91.6%, respectively. The area of cropland (including both, used and unused) in that map amounts to 9.1 Mha, similar to other studies and statistics [52,78].

Administrative boundaries from the GADM database of Global Administrative Areas, version 2.5 (http://www.gadm.org/), provided the basis for the stratification (Section 3.1). This database subdivides the study area into provinces, referred to as oblasts in Russian. Oblasts are province-level administrative units, equivalent to the NUTS-3 level in the European Union. In total, 39 provinces that correspond to the "oblast" administrative level 2 in the former Soviet Union cover the study region.

The Global Agro-Ecological Zones (GAEZ) dataset, version 3.0., which is based on the Harmonized World Soil Database (HWSD) and climate data for 1961–1990 [79,80], was taken from the Food and Agriculture Organization (FAO). It provides a description of the environmental characteristics of a region and the crop suitability index for several crop types (cotton, wheat and rice, which are the major crop types in the ASB).

2.6. Mapping Abandoned Cropland

The mapping of cropland abandonment involved two stages (Figure 5): (i) a per stratum classification of abandoned cropland following a stratified classifier and (ii) a fusion of the most accurate stratum-specific results based on pixel-level class memberships.

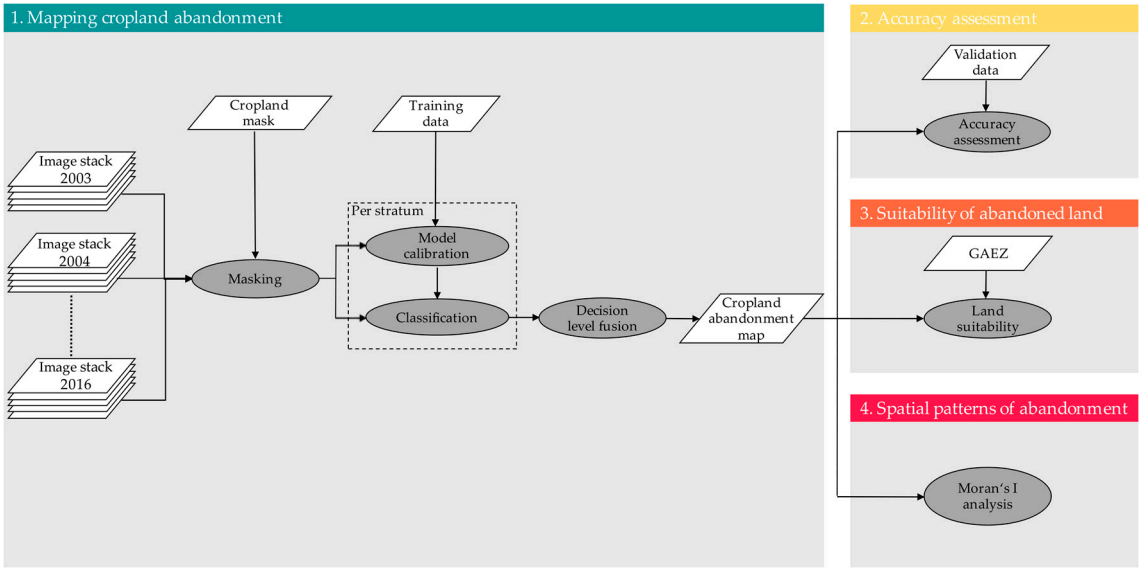

Figure 5. Scheme showing the workflow for mapping abandoned cropland using the stratified classifier (Section 3.1). The skewed rectangles represent input and output data sets, whereas ellipses represent analytical steps.

Because of the agro-ecological gradients and the variety of management practices in the ASB, spectral signatures varied spatially and could lower the recognition ability by a single global classifier. The study area, therefore, was stratified according to administrative boundaries (Section 2.5), assuming that they would either (i) tend to separate irrigation systems and thus follow the agro-ecological boundaries in some cases, or in others, (ii) provide finer spatial units of environmental zonation. A buffer zone of 100 km was assumed to minimize boundary artifacts due to the stratum-specific training. A non-stratified classifier was used as a benchmark, i.e., all training pixels were used to calibrate a global classifier model.

The classification approach (for both, with and without stratification) consisted of mapping abandoned cropland by using two classifier algorithms, random forest (RF) [81] and supported vector machines (SVM) [36]. In previous studies, both algorithms demonstrated a good ability to create accurate LULCC maps [36,82–85], specifically abandonment maps [19,29,30,33]. RF is an ensemble of decision trees (DTs) that were trained based on random, bootstrapped samples of the training data, which gave this algorithms its name [81]. DTs are non-parametric, hierarchical classifiers that predict class membership by recursively partitioning datasets into increasingly homogeneous, mutually exclusive subsets via a branched system of data splits [86]. In contrast to other classifier algorithms, which use the whole feature space at once and make a single membership decision, SVMs [87] only require the most informative samples to make the class decision [88] and they are relatively insensitive to high-dimensional datasets [89]. SVMs are based on the notion of separating classes into a higher dimensional features (Hilbert) space by fitting an optimal separating hyperplane (OSH) between them, focusing on those training samples that lie at the edge of the class distributions, the so-called support vectors [90]. Despite their high accuracies, RF and SVM might result in complementary results, which can be overcome by decision fusion [7,36,91,92].

During the classification process, subsets of features were randomly generated from the full input data set, i.e., 50% of the 448 features (6 annual NDVI metrics plus 26 annual NDVI values per growing season from 2003–2016, see Section 2.3).

The random generation was repeated 10 times (10 per RF and 10 per SVM), which resulted in 20 maps of abandoned vs. active cropland. These 20 maps were fused at the per stratum level, resulting in one map per stratum, similar to Löw et al. [36]. The selection of input features (we tested

10%, 20%, . . . , 100%) and number of iterations (we tested 10, 20, 50 and 100 iterations) was assessed empirically and confirmed by similar studies using random feature selection [36,93].

The fusion considers the probabilistic a-posteriori values estimating class membership at the pixel level by the RF [94] and the SVM [95]. Depending on the algorithm, the way these "softened" outputs are calculated differ from each other: in the RF framework, it is defined as the number of trees in the RF ensemble voting for the final class [94], in SVM classification, it is based on the distances of the samples to the OSH in the feature space [95,96]. Previous studies found that high (low) a-posteriori values from both algorithms are correlated with correctly (incorrectly) classified test pixels and are comparable with each other [94–96]. Further, the decision fusion assesses the reliability of each map based on its per-class accuracy and according to the method of [36].

The number of trees in the RF was set to 500 because a higher number did not increase accuracy or the number of random split variables to the square root of the number of input variables [83]. Training of the SVM includes choosing the kernel parameter γ and the regularization parameter C [97], which was done using a systematic grid search in 2-D space that is spanned by γ and C, using a threefold cross-validation. The range of γ was [0.00125, 10]; the range of C was finally set to [1, 200]. The widely used radial basis function (RBF) kernel was selected in this study since linear or polynomial kernels were tested but resulted in lower accuracies (not reported here).

The delineation of a 100 km-buffer around the strata resulted in an overlap of the stratum-specific maps. Therefore, the maps were fused by using the per-pixel class memberships from the RF and SVM algorithms. For each pixel in the overlapping regions of the strata, several possible class outputs were combined by assigning weights to the class decision of each method in proportion to its corresponding classification accuracy per stratum. The decision of a method t is defined as $d_{t,j} \in \{0,1\}$, with $t = 1,\ldots,T$ and class $j = 1,\ldots,C$, where T is the number of methods or classifiers and C is the number of classes (here: 2). If t chooses class ω_j, then $d_{t,j} = 1$ and 0 otherwise [92]. The final classification is then determined by the following:

$$\sum_{t=1} \omega_t d_{t,J} = max_{j=1}^{C} \sum_{t=1} \omega_t d_{t,j} \quad (1)$$

that is, if the total weighted vote received by ω_j is higher than the total weighted vote received by any other class. Weights ω_t to t are defined by the overall classification accuracy of t. In areas without overlap, a fusion was not possible and the final class corresponded to the stratum-specific classification available.

2.7. Accuracy Assessment

The accuracy of the maps was systematically assessed with an independent subset of the reference dataset (Section 2.4). For each active vs. abandoned map, a confusion matrix was calculated at the province level [98,99] and included the overall accuracy, user's accuracy and producer's accuracy. As recommended [100], the overall accuracy measures were reported using 95% confidence intervals [101]. The confidence interval (CI) of the difference (inequality) in accuracy values between two classifier algorithms is given as follows:

$$p_1 - p_0 \pm z_{\alpha/2} SE_{p_1 - p_0} \quad (2)$$

where $SE_{p_1-p_0}$ is the standard error of the difference between two estimated proportions with z = 1.96 and α = 0.05. The values p_1 and p_0 are the proportions of correctly classified test pixels of two classifiers under comparison. In addition, receiver operating characteristic (ROC) curves and the corresponding AUC have been calculated; the AUC is an increasingly used accuracy metric in machine-learning and data mining [102–104]. The AUC ranges from 0–100%, with 100% representing an error-free classification. As a random classification yields an AUC of 50%, no realistic classification should have

an inferior AUC [104]. By averaging the AUC over the different classes, an overall measure for the quality of the model predictions is obtained [94]:

$$AUC_{avg} = \sum_{i=1}^{c} AUC(i) * w(i) \quad (3)$$

where c is the number of classes (here, $c = 2$), AUC(i) is the area under the ROC curve for land-cover class i and $w(i)$ is the weighing factor associated with class i. This weighing factor is determined with respect to the contribution of each class in the test dataset.

To estimate the share of abandoned land, the map was first reprojected to Asia North Albers Equal Area Conic (ESRI: 102025). We quantified uncertainty by reporting confidence intervals for accuracy and area parameters by following recommendations of [100,105–107].

2.8. Analysis of the Spatial Patterns of Abandoned and Actively Cultivated Irrigated Cropland

Hotspots of abandonment and actively cultivated cropland were identified based on developed maps by computing the area fraction of abandoned pixels within hexagons of 7.5 km diameter relative to the total cropland area in these cells [30]. Moran's I was calculated as a local indicator of the spatial autocorrelation [108] and the location of the spatial clusters of autocorrelation, i.e., where observations with high (abandoned cropland) or low (active cropland) value clusters or spatial outliers were identified. The significance of the detected hotspots of abandoned and actively cultivated cropland was assessed using a one-sided t-test at 5% and 1% significance levels [109].

To map the patterns of abandoned farmland across the entire ASB, first, the percentage of abandoned irrigated cropland was compared to the total agricultural land based on the agricultural land mask [71] within each country of the study region. Next, the abandonment rate was estimated as the percentage of abandoned cropland relative to the sum of abandoned plus active irrigated cropland. Then, the abandonment rates were summarized by administrative units (provinces).

Finally, the abandonment rates were compiled by biophysical suitability for agriculture using the crop suitability index from the GAEZ. Therefore, the crop suitability index for the most dominating crops in the region (e.g., cotton, wheat and rice) was selected for intermediate input levels [79,80] of irrigated crop production in the region. These were defined as farming systems that are partly market oriented, medium labor intensive, with the use of some fertilizer application and chemical pest disease and weed control [79,80]. Abandonment rates were summarized for seven discrete classes of each crop suitability index and for unique combinations of province/country-level administrative units.

3. Results

3.1. Classification Accuracies

The stratified classifier approach yielded maps (Figure 6) with an overall accuracy of 0.879 (LI 0.864, UI 0.892), which was statistically more accurate ($p < 0.05$) than the global classification approach, at 0.811 (LI 0.790, UI 0.831) [101]. Accordingly, the AUC of the stratified classifier (0.867) was higher than the AUC of the global classifier (0.840). Overall, these AUC values indicate a good performance compared to that of a random classifier. High per-class accuracies were attained with the stratified classification approach (Table 3): active cropland was mapped with 0.879 UA and 0.924 PA, abandoned cropland was mapped with 0.877 UA and 0.810 PA.

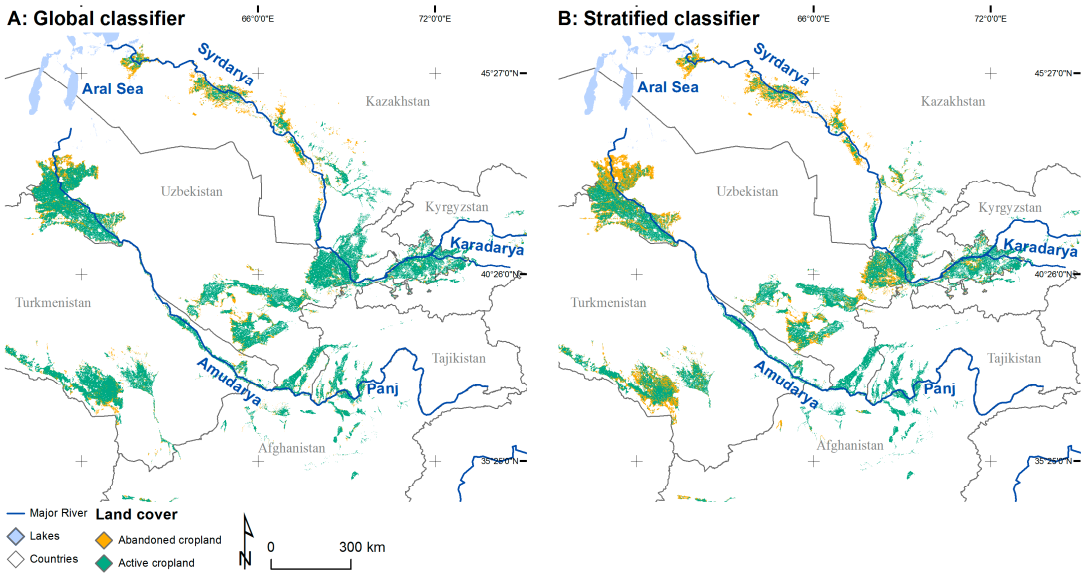

Figure 6. Comparison of the map of abandoned irrigated cropland for the global (left) and stratified (right) classifier method.

Table 3. Comparison of the area under receiver operator curves and the overall, user's and producer's accuracies. Lower (LI) and upper (UI) values indicate the 95% confidence intervals (CI) of the overall accuracy.

		Global Classifier	Stratified Classifier
Area under ROC		0.840	0.867
Overall accuracy		0.811	0.879
Lower 95% CI		0.790	0.864
Upper 95% CI		0.831	0.892
Active	User's accuracy	0.790	0.879
	Producer's accuracy	0.877	0.924
Abandoned	User's accuracy	0.840	0.877
	Producer's accuracy	0.734	0.810

The classification accuracies varied widely across strata (provinces) (Table 4). The range between the maximum and minimum overall accuracies across provinces was 0.18, compared to 0.26 for the unstratified approach (not shown here). Less accurate results occurred for the abandoned cropland class in some of the downstream regions, e.g., southern Kazakhstan (0.70) or Karakalpakstan (0.77), while the highest and higher accuracies were achieved for the active cropland class. In 9 out of 39 cases, the global classifier was more accurate than the global classifier without stratification. In 13 out of 30 cases, when the stratified classifier was more accurate, this difference was statistically significant ($p < 0.05$). For example, the highest differences were found in Qyzylorda (0.16), southern Kazakhstan (0.13), Tashauz (0.20) and Karakalpakstan (0.15).

Table 4. Overall, producer's and user's accuracies of abandoned and active cropland across 39 administrative level-II regions (provinces) in six countries of the Aral Sea Basin, based on the *stratified classifier* method.

Country	Province	Overall Accuracy	UI	LI	AUC	Abandoned		Active	
						Producer	User	Producer	User
Afghanistan	Badakhshan	0.85	0.90	0.78	0.83	0.88	0.78	0.90	0.74
	Badghis	0.65	0.78	0.51	0.58	0.88	0.29	0.67	0.60
	Baghlan	0.83	0.90	0.73	0.77	0.92	0.62	0.85	0.76
	Balkh	0.70	0.77	0.63	0.63	0.87	0.39	0.72	0.63
	Bamyan	1.00	1.00	0.66	1.00	1.00	1.00	1.00	1.00
	Faryab	0.59	0.69	0.49	0.54	0.87	0.22	0.60	0.56
	Jawzjan	0.58	0.68	0.47	0.52	0.89	0.15	0.59	0.50
	Kunduz	0.79	0.85	0.71	0.75	0.89	0.62	0.80	0.77
	Samangan	0.74	0.83	0.64	0.71	0.94	0.48	0.71	0.86
	Sari Pul	0.53	0.63	0.42	0.52	0.87	0.16	0.53	0.54
	Takhar	0.85	0.90	0.78	0.83	0.89	0.77	0.90	0.75
Kazakhstan	Qyzylorda	0.96 *	0.98	0.94	0.96	0.94	0.98	0.98	0.94
	South Kazakhstan	0.92 *	0.95	0.89	0.93	0.90	0.95	0.96	0.87
Kyrgyzstan	Batken	0.94	0.97	0.87	0.93	0.95	0.90	0.96	0.88
	Jalal-Abad	0.97	0.99	0.93	0.97	0.96	0.98	0.99	0.89
	Naryn	0.90	0.95	0.83	0.89	0.91	0.88	0.97	0.71
	Osh	0.90	0.95	0.83	0.89	0.91	0.88	0.97	0.71
Tajikistan	Dushanbe	0.90	0.95	0.83	0.94	0.88	1.00	1.00	0.61
	Gorno-Badakhshan	0.84	0.90	0.76	0.82	0.87	0.76	0.88	0.74
	Khatlon	0.79	0.85	0.73	0.74	0.85	0.63	0.87	0.58
	Leninabad	0.93	0.96	0.90	0.92	0.95	0.88	0.95	0.88
Turkmenistan	Ashgabat	0.85 *	0.88	0.82	0.85	0.96	0.74	0.81	0.94
	Chardzhou	0.87 *	0.89	0.85	0.86	0.95	0.76	0.85	0.92
	Mary	0.85 *	0.88	0.82	0.84	0.95	0.72	0.81	0.92
	Balkan	0.95 *	0.97	0.93	0.95	0.95	0.96	0.96	0.94
	Tashauz	0.96 *	0.99	0.92	0.96	0.96	0.96	0.99	0.86
Uzbekistan	Andijon	0.93	0.96	0.88	0.93	0.94	0.91	0.93	0.92
	Bukhoro	0.97 *	0.99	0.92	0.97	0.96	0.97	0.99	0.89
	Ferghana	0.93	0.96	0.89	0.92	0.95	0.90	0.94	0.92
	Jizzakh	0.96 *	0.98	0.95	0.96	0.95	0.98	0.98	0.95
	Karakalpakstan	0.94 *	0.97	0.90	0.93	0.98	0.88	0.93	0.96
	Kashkadarya	0.98	1.00	0.95	0.99	0.97	1.00	1.00	0.96
	Khorezm	0.97 *	0.99	0.92	0.97	0.97	0.97	0.99	0.93
	Namangan	0.94	0.96	0.92	0.94	0.93	0.96	0.97	0.91
	Navoi	0.94 *	0.96	0.90	0.93	0.96	0.91	0.94	0.93
	Samarkand	0.92 *	0.96	0.86	0.90	0.94	0.86	0.94	0.86
	Sirdaryo	0.70	0.78	0.61	0.60	0.84	0.35	0.77	0.46
	Surkhandarya	0.91	0.95	0.86	0.91	0.93	0.89	0.94	0.87
	Tashkent	0.94 *	0.97	0.91	0.94	0.97	0.90	0.93	0.96
	Median	0.91	0.95	0.85	0.91	0.94	0.88	0.94	0.87
	Average	0.86	0.91	0.80	0.85	0.93	0.77	0.88	0.81

* indicates that the stratified classifier is more accurate (according to overall accuracy) than the global classifier and that the difference is statically significant ($p < 0.05$).

3.2. Spatial Patterns of Abandoned Irrigated Cropland

Analysis of the cropland abandonment map revealed that abandonment occurred in all provinces investigated (Figure 7). In total, 13% (1.15 Mha; error-adjusted) of the observed irrigated cropland (8.86 Mha; error-adjusted) was abandoned in 2016 (Table 5). The 95% CIs of the abandoned cropland were narrow, ranging from <0.001 (0.000128 Mha) to 0.009 (0.437 Mha), with an average of 0.002 (Table 5).

The largest share of abandoned area occurred in the provinces of Kazakhstan (38% of the cropland), followed by Turkmenistan (14%), Uzbekistan (13%), Kyrgyzstan (13%) and Afghanistan (11%). The lowest rates were found in Tajikistan (7%). The highest proportion of abandoned cropland occurred in Kyzyl-Orda in Kazakhstan (49%) and Karakalpakstan in Uzbekistan (40%), whereas the densely populated provinces Fergana, Dushanbe, Tashkent and Surkhandarja showed the lowest shares of abandonment (below 10% each). Hotspots of abandoned cropland occurred particularly in

the downstream regions of Uzbekistan (e.g., Karakalpakstan) and Kazakhstan (e.g., Kazalinsk and Kyzyl-Orda) and partially in some upstream regions in Uzbekistan (e.g., Kashkadarja, 16%) (Figure 8).

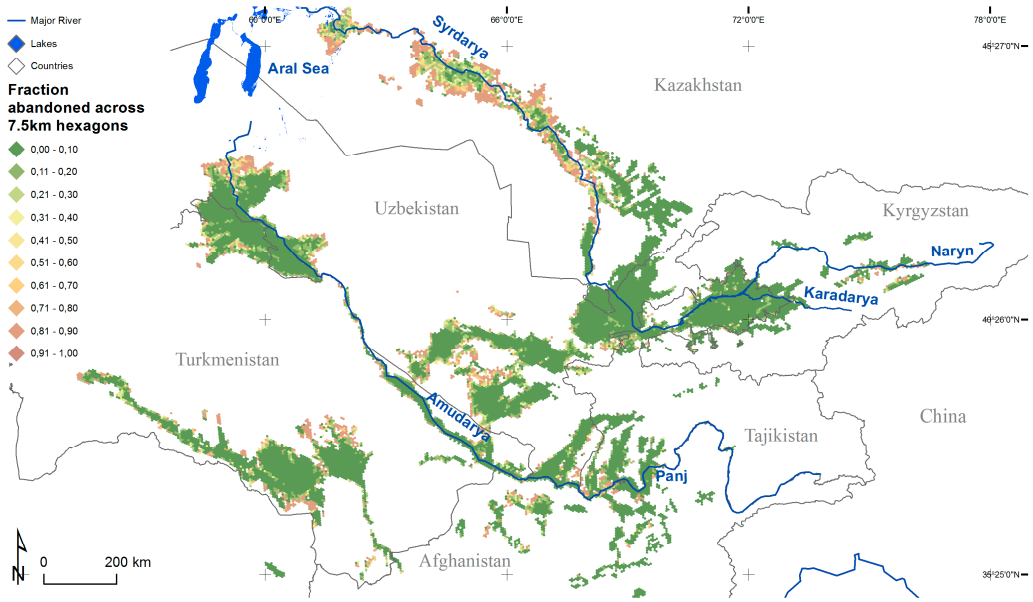

Figure 7. Map of abandoned irrigated cropland (for 2016) in six countries of the Aral Sea Basin as derived by the stratified classifier method.

Table 5. Estimates of the proportion of abandoned irrigated cropland to the total cropland in 39 administrative level-II regions (provinces) in six countries of the Aral Sea Basin and error-adjusted area estimates with 95% confidence intervals.

Country	Province	Proportion Abandoned	95% Confidence Interval
Afghanistan	Badakhshan	0.08	0.009
	Badghis	0.14	0.004
	Baghlan	0.09	0.002
	Balkh	0.16	0.001
	Bamyan	0.08	<0.001
	Faryab	0.09	0.009
	Jawzjan	0.23	0.002
	Kunduz	0.12	0.002
	Samangan	0.05	<0.001
	Sari Pul	0.15	0.002
	Takhar	0.09	0.001
Kazakhstan	Qyzylorda	0.49	<0.001
	South Kazakhstan	0.20	0.001
Kyrgyzstan	Batken	0.14	0.001
	Jalal-Abad	0.15	0.004
	Naryn	0.15	<0.001
	Osh	0.12	0.011
Tajikistan	Dushanbe	0.03	0.002
	Gorno-Badakhshan	0.05	<0.001
	Khatlon	0.09	0.001
	Leninabad	0.11	<0.001
Turkmenistan	Ashgabat	0.10	<0.001
	Chardzhou	0.12	<0.001
	Mary	0.12	<0.001
	Balkan	0.26	<0.001
	Tashauz	0.14	0.001

Table 5. *Cont.*

Country	Province	Proportion Abandoned	95% Confidence Interval
Uzbekistan	Andijon	0.05	<0.001
	Bukhoro	0.14	0.001
	Ferghana	0.05	<0.001
	Jizzakh	0.11	<0.001
	Karakalpakstan	0.40	0.001
	Kashkadarya	0.16	0.001
	Khorezm	0.09	0.001
	Namangan	0.07	<0.001
	Navoi	0.18	0.001
	Samarkand	0.09	0.002
	Sirdaryo	0.06	0.002
	Surkhandarya	0.08	0.006
	Tashkent	0.06	<0.001
Median		0.11	0.001
Average		0.13	0.002

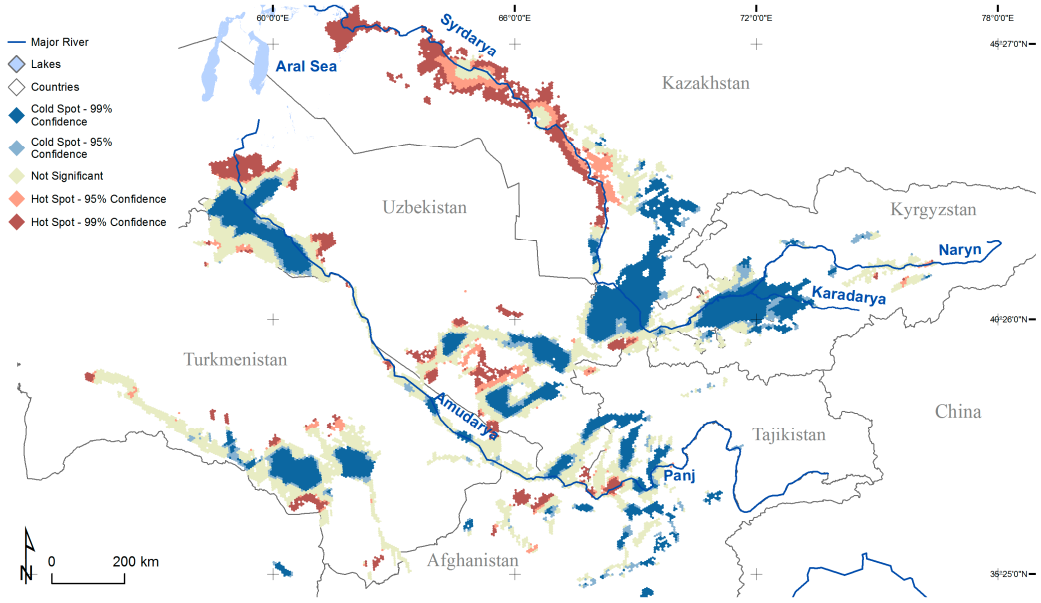

Figure 8. Hotspots of abandoned irrigated cropland (orange—95% of confidence and red color—99% of confidence) and active irrigated cropland (light blue—95% of confidence and dark blue color—99% of confidence) in the six countries of the Aral Sea Basin as derived by the *stratified classifier* method. For the correct interpretation of colors, please refer to the digital version of the manuscript.

The analysis of abandonment rates for each agricultural suitability class and for each province revealed a series of patterns (Table 6). In most provinces, higher abandonment rates emerged in the least-suitable areas for agriculture ("not suitable" or "very marginal") irrespective of three major crop classes: cotton, wheat and rice. At the same time, abandonment was also common in the provinces with medium, high and very high suitability for the cultivation of wheat production (e.g., Kyzyl-Orda, Mary, Ashgabat and Chardzou), rice (e.g., Kyzyl-Orda, Mary, Karakalpakstan and Bukhara) and cotton (e.g., Tashauz, Mary, Bukhara, Karakalpakstan, Chardzou and Samarkand).

Table 6. Abandonment rates per crop suitability class in 39 administrative level-II regions (provinces) in six countries of the Aral Sea Basin while considering medium input level irrigated crop cultivation (cotton, rice and wheat). Abandonment data were based on map estimates from the stratified classifier and suitability indices (SI) based on GAEZ 3.0 (http://gaez.fao.org). Colors are added for the sake of readability: The dark red (green) color indicates highest (lowest) abandonment rates.

Cotton

Abandonment	Afghanistan											Kazakhstan			Kyrgyzstan			Tajikistan			Turkmenistan							Uzbekistan														
	Badakhshan	Badghis	Baghlan	Balkh	Bamyan	Faryab	Jawzjan	Kunduz	Samangan	Sari Pul	Takhar	Qyzylorda	South Kazakhstan	Batken	Jalal-Abad	Naryn	Osh	Dushanbe	Gorno-Khatlon	Leninabad	Ashgabat	Chardzhou	Mary	Balkan	Tashauz	Andijon	Bukhoro	Ferghana	Jizzakh	Karakalpakstan	Kashkadarya	Khorezm	Namangan	Navoi	Samarkand	Sirdaryo	Surkhandarya	Tashkent
Very High			0.044																				0.199																		
High	0.148	0.826	0.141	0.054			0.333	0.120			0.152	0.572	0.095	0.025				0.088	0.072	0.125	0.181	0.183	0.380	0.255	0.138		0.450		0.128	0.678	0.229	0.118		0.259	0.247	0.056	0.104	0.020
Good	0.036		0.084	0.126		0.208	0.443	0.134			0.099	0.570	0.074	0.147	0.022		0.015	0.018	0.103	0.172	0.107	0.122	0.048	0.211	0.155	0.060	0.114	0.054	0.065	0.175	0.093	0.057	0.075	0.127	0.065	0.049	0.049	0.015
Medium		0.058	0.054	0.054			0.222	0.081				0.344	0.239		0.019			0.022	0.064		0.059	0.061	0.070		0.117	0.034	0.179	0.006	0.041	0.468	0.161	0.043	0.039	0.005	0.044		0.041	
Moderate		0.124	0.042	0.116			0.208	0.091		0.164		0.450	0.116		0.008		0.039		0.221		0.071	0.088	0.066		0.082	0.041	0.103			0.290			0.087		0.024		0.042	
Marginal			0.017	0.285			0.234	0.030													0.111	0.147	0.109		0.212		0.424			0.289		0.104					0.000	
Very marginal			0.017								0.071			0.061	0.009	0.284	0.015			0.186		0.199					0.127						0.095					0.159
Not suitable	0.266	0.039	0.051		0.010	0.174	0.711		1.000	0.163	0.791	0.210	0.108	0.009	0.150		0.114		0.163	0.435	0.358	0.289	0.443	0.303	0.326	0.288	0.577	0.444	0.303	0.788	0.341	0.297	0.277	0.746	0.413		0.323	0.038

Rice

Abandonment	Badakhshan	Badghis	Baghlan	Balkh	Bamyan	Faryab	Jawzjan	Kunduz	Samangan	Sari Pul	Takhar	Qyzylorda	South Kazakhstan	Batken	Jalal-Abad	Naryn	Osh	Dushanbe	Gorno-Badakhshan	Khatlon	Leninabad	Ashgabat	Chardzhou	Mary	Balkan	Tashauz	Andijon	Bukhoro	Ferghana	Jizzakh	Karakalpakstan	Kashkadarya	Khorezm	Namangan	Navoi	Samarkand	Sirdaryo	Surkhandarya	Tashkent
Very			0.0	0.05			1.00					0.47	0.27								0.21	0.19	0.09	0.19					1.00	0.69					0.08		0.13	0.08
High			0.0				0.33	0.00			0.13	0.50	0.16	0.01			0.05	0.02		0.06	0.23	0.17	0.18	0.28	0.28		0.25	0.45	0.11	0.14	0.52	0.24		0.25	0.09	0.05	0.09	0.01
Good	0.02	0.058	0.2	0.31			0.26	0.25			0.14	0.49	0.08	0.02	0.05		0.04	0.03		0.07	0.10	0.08	0.06	0.10	0.17	0.32	0.21		0.14	0.04	0.11	0.12	0.11	0.10	0.03	0.06	0.10	0.09	0.03
Medium	0.03	0.826	0.0	0.14			0.60	0.09			0.12		0.08	0.02	0.02		0.01	0.01		0.07	0.14	0.13	0.10	0.10	0.10			0.22	0.12		0.29	0.11		0.12	0.39		0.04	0.03	0.00
Moderat			0.0	0.12		0.028	0.21	0.09			0.45	0.07	0.71	0.01	0.17	0.01		0.01	0.02		0.26	0.14	0.02	0.23	0.05	0.09	0.04		0.08	0.03	0.07	0.16	0.07	0.05	0.05	0.09		0.03	0.02	0.01
Marginal		0.124	0.0	0.09			0.24	0.04			0.12	0.00	0.56		0.26	0.01		0.01			0.26	0.15	0.14	0.18	0.12				0.37	0.07		0.28	0.42	0.10	0.08			0.13	
Very			0.0									0.11			0.42		0.28	0.01	0.04			0.36	1.00		0.19	0.35			0.16										
Not suitable		0.266	0.0	0.05		0.010	0.17	0.71		1.00	0.16	0.79	0.21	0.10	0.00	0.15		0.11		0.16	0.43	0.35	0.28	0.44	0.32	0.28	0.30	0.57	0.44	0.30	0.78	0.34	0.29	0.27	0.74	0.41		0.32	0.03

Wheat

Abandonment	Badakhshan	Badghis	Baghlan	Balkh	Bamyan	Faryab	Jawzjan	Kunduz	Samanga	Sari Pul	Takhar	Qyzylorda	South Kazakhst	Batken	Jalal-Abad	Naryn	Osh	Dushanbe	Gorno-	Khatlon	Leninabad	Ashgabat	Chardzhou	Mary	Balkan	Tashauz	Andijon	Bukhoro	Ferghana	Jizzakh	Karakalpakstan	Kashkadarya	Khorezm	Namangan	Navoi	Samarkand	Sirdaryo	Surkhandarya	Tashkent
Very	0.02		0.05								0.14	0.81	0.02	0.03	0.01	0.10	0.01	0.00		0.08	0.16			0.19				0.11	0.30		0.01		0.09		0.11			0.07	
High	0.01	0.82	0.17	0.10		0.20	0.40	0.10			0.11	0.57	0.08	0.17	0.01	0.30	0.02	0.02		0.08	0.14	0.15	0.19	0.10	0.17	0.05	0.13	0.04	0.06	0.21	0.16	0.07	0.05	0.19	0.14	0.04	0.04	0.01	0.25
Good		0.11	0.06	0.07		0.00	0.19	0.10		0.16	0.00	0.44	0.23		0.02					0.05		0.06	0.10	0.07	0.10	0.05	0.20	0.06	0.00	0.22	0.10	0.03	0.03	0.00	0.03	0.10	0.19		
Medium		0.05	0.01	0.27			0.43	0.25				0.34	0.19		0.00					0.24		0.18	0.07	0.10	0.08				0.09			0.10		0.09		0.07		0.21
Moderate			0.01	0.29			0.23	0.02					0.05									0.15	0.07	0.08	0.52		0.60		0.16	0.32		0.11					0.01		
Marginal			0.04													0.22								0.19															
Very marginal			0.04																					0.19															
Not suitable		0.26	0.03	0.05		0.01	0.17	0.71		1.00	0.16	0.79	0.21	0.10	0.00	0.15		0.11		0.16	0.43	0.35	0.28	0.44	0.32	0.28	0.57	0.44	0.30	0.78	0.34	0.29	0.27	0.74	0.41		0.32	0.03	0.30

4. Discussion

In this study, we provide the first consistent spatial analysis of post-Soviet cropland abandonment across the ASB in Central Asia. Despite a high demand for agricultural land in this region, the findings revealed widespread abandonment in the ASB area. In general, we achieved high classification accuracy for the spectrally complex change classes, such as actively cultivated and abandoned cropland in drylands (overall accuracy = 0.879, AUC = 0.867).

This study revealed that the stratification-based classification with a fusion of the classification results with RF and SVM classifiers were statistically more accurate than non-stratified single classifications (either with SVM or RF) at $p < 0.05$. Our findings regarding the more accurate performance using stratification-based classifications may be highly relevant for subnational- to continental-scale classification efforts [46,47], which often suffer from a lack of accurate generalization of training signatures across large areas with non-parametric machine-learning classifiers [35,110,111]. For instance, in one of the preceding works where one of the authors was involved [35], the difficulty of creating an accurate land-cover classification across Eastern Europe was attributed to a lack of spectral signature generalization by a single non-parametric machine-learning classifier (SVM). This is particularly relevant for the classes, such as abandoned agricultural land, which may represent multiple stages of vegetation succession depending on the period of abandonment and biophysical conditions (sparse vegetation, grasses, shrubs and trees). Despite the overall superiority of non-parametric machine-learning classifiers compared to parametric ones (e.g., the maximum likelihood classifier) [112,113], machine-learning classifiers may not fully overcome the complexity of mapped land-use change classes, such as land abandonment. Thus, additional efforts are required to boost the classification accuracies in order to make the land-cover change products suitable for other applications [112]; the fusion of classification methods and stratified classification approaches tested here is one example. It should be noted, however, that stratification-based classification approaches might require more training samples than non-stratified classifiers. Therefore, they may not be recommendable if the training sample size is small, or techniques would have to be employed to artificially increase the training set size and regenerate the native class proportions in the training set [114].

Our method does not provide information about the timing of land abandonment, which would be challenging due to the intermittent fallow phases that are triggered by droughts or management practices. Our method, given that reference data could be made available, could be extended to annual land cover mapping and to assessing land cover trajectories for assessing the abandonment year, as well as for the identification of the period when land became recultivated [30]. In addition, the data set is suitable to assess the determinants of abandonment at the region level [16,115,116].

Certain factors may have contributed to some uncertainties in the estimates of the abandonment extent. For instance, the cropland mask had an overall accuracy of 89.8%, thereby contributing additional discrepancies to the land-cover estimates. By carefully checking the error matrix, we noticed the classification errors were primarily related to misclassifications between cropland and grassland/pasture classes. The latter is a dominant class across Central Asia and may thus possess a large extent of misclassified classes. Similarly, within a cropland mask, the inclusion of natural grasslands/pastures could be a source of misclassification of abandoned land due to spectral similarities, as previously reported [117]. Therefore, the map of abandoned cropland may include some permanent grasslands or shrublands, as they occur in the floodplains of Kyzyl-Orda or in the mountainous regions. We also found that in some cases, shrubland had been confused with active cropland, such as cotton [73], which was reflected in the lower producer's accuracies for "abandoned, irrigated cropland" in the downstream regions, where shrub encroachment on abandoned fields prevails. Nevertheless, the estimated abandonment rates matched well with previous small case studies in the ASB. For example, in the Kyzyl-Orda region, the estimate abandonment rate was 50% according to [7], while the current study found a rate of 49%. In addition, the total cropland area (8.86 Mha error-adjusted) matches well with other sources: 8.4 Mha [78], 8.5 Mha [55], or 8.19 Mha [118].

The error-adjusted share of cropland abandonment (ca. 13%) falls within the range observed for other regions of the former Soviet Union. For instance, the farmland abandonment rate of 18% detected with a MODIS time series has been observed during 2006–2008 across Russia, Poland, Belarus, Estonia, Latvia, Lithuania and the Ukraine [29]. While the direct comparison of land abandonment rates and patterns with other case studies across former Soviet Union is challenging because the time periods and abandonment definitions used vary among studies, the cross-border comparison in the ASB area revealed some interesting patterns, similar to cross-border studies in Eastern Europe [119,120]. For instance, our study revealed drastic differences in land abandonment rates among the neighboring countries (i.e., 4% in Kyrgyzstan and 33% in Kazakhstan) compared to variations in land abandonment rates at the province level within the studied countries. Kazakhstan and Kyrgyzstan were once part of the Soviet Union. After the breakup of the Soviet Union, they followed common pathways from a state-controlled economy toward a market economy. However, the land tenure regimes differed in Kazakhstan and Kyrgyzstan and the share of agriculture in the gross domestic product and the share of the rural population also differed. By 2014, the agriculture value in land-rich Kazakhstan added to the total GDP, comprising only 4.7% of the total GDP, in contrast to land-scarce Kyrgyzstan, with 17.1% of the total GDP. In 2014, the share of the rural population was 47% in Kazakhstan and 67% in Kyrgyzstan. Additionally, until recently, private ownership was not allowed in Kazakhstan and there was a non-functioning land market, thus creating preconditions of inefficient land use and higher abandonment rates, in contrast to neighboring Kyrgyzstan, where private land ownership was allowed (Table 1).

Overall, land abandonment rates across other Central Asian countries in the ASB (Turkmenistan, Tajikistan and Uzbekistan) were much lower than those in the other post-Soviet states (e.g., Kazakhstan and Russia) possibly because of the high rural population density and a higher value added to agriculture in the total GDP (Table 1). In Uzbekistan, we found more abandoned cropland in agro-environmentally marginal regions (e.g., Karakalpakstan [121]) than in Kazakhstan or Turkmenistan. The differences in land abandonment rates in cross-border Tajikistan and Kyrgyzstan were less pronounced than in Kazakhstan and Kyrgyzstan. The Central Asian countries, except for Kazakhstan, developed regional food sovereignty (security) policies to ensure sufficient food production and supply land-scarce regions with fast-growing populations after 1991. We do not elaborate here on the case of Afghanistan due to an ongoing civil war, which dramatically shapes agricultural production and different forms of land tenure [122]. Despite skyrocketing population growth, insurgencies and armed conflict with internally displaced peoples and refugees may cause land abandonment.

We also found moderate rates of cropland abandonment on agricultural lands suited for crop production in Kazakhstan and Kyrgyzstan (Table 6). The observed pattern of cropland abandonment in Kazakhstan may reflect the consequences of the transition to a market economy, i.e., privatization of the agricultural sector that has occurred in Kazakhstan after independence in 1991 [123,124]. Kyzyl-Orda, for instance, is a region with a strong reputation for rice production but statistics illustrate that rice production areas in Kazakhstan have dropped from approximately 110,000 ha to 65,000 ha during the period 1993–2002 and then increased to an average of 91,200 ha during the period 2009–2013 (http://faostat3.fao.org; last access, 1 January 2016). Such statistics may be interpreted as the parts of the cultivated land identified in this study that had already been recultivated during the past decade and where the previous decisions and production inputs of the landowners, e.g., during the privatization process, could have also been of influence. Other drivers, such as population dynamics, employment structures, or others, may have played a role [123] but further studies are needed to interpret the spatial patterns of the abandoned cropland.

5. Conclusions

Understanding the patterns of agricultural abandonment is important because abandonment affects ecosystem services and land availability suited for different land uses in various ways and is thus important for land-use planning. The map of abandoned cropland provides a suitable data set for

such research. In contrast to previous studies, our study showed that abandonment is also common in areas where land demand is high (e.g., on irrigated lands in the ASB of Central Asia). In total, 13% (1.15 Mha) of the irrigated agricultural land was abandoned by 2016, with a drastic difference in rates across the countries. Despite ongoing recultivation, some abandoned lands represent the agricultural potential not only for looming land scarcity in Central Asia but also for alternative land-use. Here, we also tested and proved that a MODIS time series is well suited to tracking abandonment in arid areas where the difference between actively cultivated and abandoned cropland is subtle. The overall accuracy of the stratum-adjusted classification (87.9%) was more accurate compared to unstratified classifications. The map of abandoned irrigated cropland provides a novel basis and the necessary baseline information to guide land-use and conservation planning support in the region, such as the assessment of environmental trade-offs and social constraints of recultivation.

Acknowledgments: We thank for the support the International Centre for Agricultural Research in Dry Areas (ICARDA). We also acknowledge funding from the German Federal Ministry of Food and Agriculture (BMEL), the Federal Office for Agriculture and Food (BLE) (project GERUKA) and the Volkswagen Foundation (project BALTRAK). We also thank the German Technical Cooperation (GIZ) for supporting field trips to Karakalpakstan in 2008 and 2009, Murod Khamalov for providing ground reference data from Karakalpakstan and Marat Nagmetullayev (GIZ) for providing ground reference data from Kyzyl-Orda, and ICARDA for providing reference data in 2014. This work has also been performed via the OpenLab initiative, which is funded by the Russian Government Program of Competitive Growth of Kazan Federal University.

Author Contributions: F.L., F.W., O.D. and A.V.P. conceived and designed the experiments; F.L. and F.W. performed the experiments; F.L., C.B., A.A. and F.W. analyzed the data; All co-authors substantially contributed to writing the paper.

Conflicts of Interest: The authors declare no conflict of interest.

References

1. Alexandratos, N.; Bruinsma, J. *World Agriculture: Towards 2030/2050—The 2012 Revision (Report)*; FAO: Rome, Italy, 2012.
2. Erb, K.H.; Haberl, H.; Jepsen, M.R.; Kuemmerle, T.; Lindner, M.; Müller, D.; Verburg, P.H.; Reenberg, A. A conceptual framework for analysing and measuring land-use intensity. *Curr. Opin. Environ. Sustain.* **2013**, *5*, 464–470. [CrossRef] [PubMed]
3. Sadras, V.O.; Cassman, K.G.G.; Grassini, P.; Hall, A.J.; Bastiaanssen, W.G.M.; Laborte, A.G.; Milne, A.E.; Sileshi, G.; Steduto, P. *Yield Gap Analysis of Field Crops, Methods and Case Studies*; FAO Water Reports 41; FAO: Rome, Italy, 2015.
4. Foley, J.A.; Ramankutty, N.; Brauman, K.; Cassidy, E.S.; Gerber, J.S.; Johnston, M.; Mueller, N.D.; O'Connell, C.; Ray, D.K.; West, P.C.; et al. Solutions for a cultivated planet. *Nature* **2011**, *478*, 337–342. [CrossRef] [PubMed]
5. Lobell, D.B.; Cassman, K.G.; Field, C.B.; Field, C.B. Crop Yield Gaps: Their Importance, Magnitudes, and Causes. *Annu. Rev. Environ. Resour.* **2009**, *34*, 179–204. [CrossRef]
6. Qadir, M.; Noble, A.D.; Qureshi, A.S.; Gupta, R.K.; Yuldashev, T.; Karimov, A. Salt induced land and water degradation in the Aral Sea basin: A challenge to sustainable agriculture in Central Asia. *Nat. Resour. Forum* **2009**, *33*, 134–149. [CrossRef]
7. Löw, F.; Fliemann, E.; Abdullaev, I.; Conrad, C.; Lamers, J.P.A. Mapping abandoned agricultural land in Kyzyl-Orda, Kazakhstan using satellite remote sensing. *Appl. Geogr.* **2015**, *8*, 377–390. [CrossRef]
8. Dubovyk, O.; Menz, G.; Conrad, C.; Kan, E.; Machwitz, M.; Khamzina, A. Spatio-temporal analyses of cropland degradation in the irrigated lowlands of Uzbekistan using remote-sensing and logistic regression modeling. *Environ. Monit. Assess.* **2013**, *185*, 4775–4790. [CrossRef] [PubMed]
9. Sommer, R.; Glazirina, M.; Yuldashev, T.; Otarov, A.; Ibraeva, M.; Martynova, L.; Bekenov, M.; Kholov, B.; Ibragimov, N.; Kobilov, R.; et al. Impact of climate change on wheat productivity in Central Asia. *Agric. Ecosyst. Environ.* **2013**, *178*, 78–99. [CrossRef]
10. Horion, S.; Prishchepov, A.V.; Verbesselt, J.; de Beurs, K.; Tagesson, T.; Fensholt, R. Revealing turning points in ecosystem functioning over the Northern Eurasian agricultural frontier. *Glob. Chang. Biol.* **2016**, *22*, 2801–2817. [CrossRef] [PubMed]

11. Pervez, S.M.; Budde, M.; Rowland, J. Mapping irrigated areas in Afghanistan over the past decade using MODIS NDVI. *Remote Sens. Environ.* **2014**, *149*, 155–165. [CrossRef]
12. Bernauer, T.; Siegfried, T. Climate change and international water conflict in Central Asia. *J. Peace Res.* **2012**, *49*, 227–239. [CrossRef]
13. Siegfried, T.; Bernauer, T.; Guiennet, R.; Sellars, S.; Robertson, A.W.; Mankin, J.; Bauer-Gottwein, P.; Yakovlev, A. Will climate change exacerbate water stress in Central Asia? *Clim. Chang.* **2012**, *112*, 881–899. [CrossRef]
14. Ji, C. *Central Asian Countries Initiative for Land Management Multicountry Partnership Framework Support Project Report*; Asian Development Bank: Tashkent, Uzbekistan, 2008.
15. Bekchanov, M.; Lamers, J.P.A. Economic costs of reduced irrigation water availability in Uzbekistan (Central Asia). *Reg. Environ. Chang.* **2016**, *16*, 2369–2387. [CrossRef]
16. Prishchepov, A.V.; Müller, D.; Dubinin, M.; Baumann, M.; Radeloff, V.C. Determinants of agricultural land abandonment in post-Soviet European Russia. *Land Use Policy* **2013**, *30*, 873–884. [CrossRef]
17. Ioffe, G.; Nefedova, T.; de Beurs, K.M. Land Abandonment in Russia: A Case Study of Two Regions. *Eurasian Geogr. Econ.* **2012**, *53*, 527–549. [CrossRef]
18. Meyfroidt, P.; Schierhorn, F.; Prishchepov, A.V.; Müller, D.; Kuemmerle, T. Drivers, constraints and tradeoffs associated with recultivating abandoned cropland in Russia, Ukraine and Kazakhstan (in press). *Glob. Environ. Chang.* **2016**, *37*, 1–15. [CrossRef]
19. Schierhorn, F.; Müller, D.; Beringer, T.; Prishchepov, A.V.; Kuemmerle, T.; Balmann, A. Post-Soviet cropland abandonment and carbon sequestration in European Russia, Ukraine, and Belarus. *Glob. Biogeochem. Cycles* **2013**, *27*, 1175–1185. [CrossRef]
20. Khamzina, A.; Lamers, J.P.A.; Vlek, P.L.G. Conversion of degraded cropland to tree plantations for ecosystem and livelihood benefits. In *Cotton, Water, Salts and Soums*; Martius, C., Rudenko, I., Lamers, J.P.A., Vlek, P.L.G., Eds.; Springer: Dordrecht, The Netherlands, 2012; pp. 235–248.
21. Lerman, Z.; Prikhodko, D.; Punda, I.; Sedi, D.; Serova, E.; Swinnen, J.; Sedik, D.; Serova, E.; Swinnen, J. *Turkmenistan Agricultural Sector Review*; FAO: Rome, Italy, 2012.
22. Qadir, M.; Quillérou, E.; Nangia, V.; Murtaza, G.; Singh, M.; Thomas, R.J.; Drechsel, P.; Noble, A.D. Economics of salt-induced land degradation and restoration. *Nat. Resour. Forum* **2014**, *38*, 282–295. [CrossRef]
23. Fritsch, S.; Conrad, C.; Dürbeck, T.; Schorcht, G. Mapping marginal land in Khorezm using GIS and remote sensing techniques. In *Restructuring Land Allocation, Water Use and Agricultural Value Chains. Technologies, Policies and Practices for the Lower Amudarya Region*; Lamers, J.P.A., Khamzina, A., Rudenko, I., Vlek, P.L.G., Eds.; Bonn University Press: Goettingen, Germany, 2014; pp. 167–178.
24. Dubovyk, O.; Menz, G.; Conrad, C.; Lamers, J.P.A.; Lee, A.; Khamzina, A. Spatial targeting of land rehabilitation: A relational analysis of cropland productivity decline in arid Uzbekistan. *Erdkunde* **2013**, *67*, 167–181. [CrossRef]
25. Prishchepov, A.V.; Radeloff, V.C.; Dubinin, M.; Alcantara, C. The effect of Landsat ETM/ETM+ image acquisition dates on the detection of agricultural land abandonment in Eastern Europe. *Remote Sens. Environ.* **2012**, *126*, 195–209. [CrossRef]
26. Griffiths, P.; Kuemmerle, T.; Baumann, M.; Radeloff, V.C.; Abrudan, I.V.; Lieskovsky, J.; Munteanu, C.; Ostapowicz, K.; Hostert, P. Forest disturbances, forest recovery, and changes in forest types across the carpathian ecoregion from 1985 to 2010 based on landsat image composites. *Remote Sens. Environ.* **2014**, *151*, 72–88. [CrossRef]
27. Radoux, J.; Chomé, G.; Jacques, D.C.; Waldner, F.; Bellemans, N.; Matton, N.; Lamarche, C.; D'Andrimont, R.; Defourny, P. Sentinel-2's potential for sub-pixel landscape feature detection. *Remote Sens.* **2016**, *8*, 488. [CrossRef]
28. Valero, S.; Morin, D.; Inglada, J.; Sepulcre, G.; Arias, M.; Hagolle, O.; Dedieu, G.; Bontemps, S.; Defourny, P.; Koetz, B. Production of a Dynamic Cropland Mask by Processing Remote Sensing Image Series at High Temporal and Spatial Resolutions. *Remote Sens.* **2016**, *8*, 55. [CrossRef]
29. Alcantara, C.; Kuemmerle, T.; Prishchepov, A.V.; Radeloff, V.C. Mapping abandoned agriculture with multi-temporal MODIS satellite data. *Remote Sens. Environ.* **2012**, *124*, 334–347. [CrossRef]
30. Estel, S.; Kuemmerle, T.; Alcantara, C.; Levers, C.; Prishchepov, A.V.; Hostert, P.; Alcántara, C.; Levers, C.; Prishchepov, A.V.; Hostert, P.; et al. Mapping farmland abandonment and recultivation across Europe using MODIS NDVI time series. *Remote Sens. Environ.* **2015**, *163*, 312–325. [CrossRef]
31. Wardlow, B.D.; Egbert, S.L. Large-area crop mapping using time-series MODIS 250 m NDVI data: An assessment for the U.S. Central Great Plains. *Remote Sens. Environ.* **2008**, *112*, 1096–1116. [CrossRef]

32. Hentze, K.; Thonfeld, F.; Menz, G. Evaluating Crop Area Mapping from MODIS Time-Series as an Assessment Tool for Zimbabwe's "Fast Track Land Reform Programme". *PLoS ONE* **2016**, *11*, e0156630. [CrossRef] [PubMed]
33. Estel, S.; Kuemmerle, T.; Levers, C.; Baumann, M.; Hostert, P. Mapping cropland-use intensity across Europe using MODIS NDVI time series. *Environ. Res. Lett.* **2016**, *11*, 24015. [CrossRef]
34. Klein, I.; Gessner, U.; Kuenzer, C. Regional land cover mapping and change detection in Central Asia using MODIS time-series. *Appl. Geogr.* **2012**, *35*, 219–234. [CrossRef]
35. Alcantara, C.; Kuemmerle, T.; Baumann, M.; Bragina, E.V.; Griffiths, P.; Hostert, P.; Knorn, J.; Müller, D.; Prishchepov, A.V.; Sieber, A.; Radeloff, V.C. Mapping the extent of abandoned farmland in Central and Eastern Europe using MODIS time series satellite data. *Environ. Res. Lett.* **2013**, *8*, 35035. [CrossRef]
36. Löw, F.; Conrad, C.; Michel, U. Decision fusion and non-parametric classifiers for land use mapping using multi-temporal RapidEye data. *ISPRS J. Photogramm. Remote Sens.* **2015**, *108*, 191–204. [CrossRef]
37. Eklund, L.; Degerald, M.; Brandt, M.; Prishchepov, A.V.; Pilesjö, P. How conflict affects land use: agricultural activity in areas seized by the Islamic State. *Environ. Res. Lett.* **2017**, *12*, 54004. [CrossRef]
38. Japan International Cooperation Agency (JICA). *The Study on Regional Development in Karakalpakstan in the Republic of Uzbekistan (Progress Report)*; JICA: Chiyoda-Ku, Japan, 2010; Volume 130.
39. Tischbein, B.; Manschadi, A.M.; Conrad, C.; Hornidge, A.; Bhaduri, A.; Hassan, M.U.; Lamers, J.P.A.; Awan, U.K.; Vlek, P.L.G. Adapting to water scarcity: constraints and opportunities for improving irrigation management in Khorezm, Uzbekistan. *Water Sci. Technol. Water Supply* **2013**, *13*, 337–348. [CrossRef]
40. Löw, F.; Knöfel, P.; Conrad, C. Analysis of uncertainty in multi-temporal object-based classification. *ISPRS J. Photogramm. Remote Sens.* **2015**, *105*, 91–106. [CrossRef]
41. Propastin, P.; Kappas, M.; Muratova, N.R. A remote sensing based monitoring system for discrimination between climate and human-induced vegetation change in Central Asia. *Manag. Environ. Qual. Int. J.* **2008**, *19*, 579–596. [CrossRef]
42. De Beurs, K.M.; Wright, C.; Henebry, G. Dual scale trend analysis for evaluating climatic and anthropogenic effects on the vegetated land surface in Russia and Kazakhstan. *Environ. Res. Lett.* **2009**, *4*, 45012. [CrossRef]
43. Shao, Y.; Lunetta, R.S. Comparison of support vector machine, neural network, and CART algorithms for the land-cover classification using limited training data points. *ISPRS J. Photogramm. Remote Sens.* **2012**, *70*, 78–87. [CrossRef]
44. Lunetta, R.; Shao, Y. Monitoring agricultural cropping patterns across the Laurentian Great Lakes Basin using MODIS-NDVI data. *Int. J. Appl. Earth Obs. Geoinf.* **2010**, *12*, 81–88. [CrossRef]
45. Vintrou, E.; Desbrosse, A.; Bégué, A.; Traoré, S.; Baron, C.; Lo Seen, D. Crop area mapping in West Africa using landscape stratification of MODIS time series and comparison with existing global land products. *Int. J. Appl. Earth Obs. Geoinf.* **2012**, *14*, 83–93. [CrossRef]
46. Zhang, H.K.; Roy, D.P. Using the 500 m MODIS land cover product to derive a consistent continental scale 30 m Landsat land cover classification. *Remote Sens. Environ.* **2017**, *197*, 15–34. [CrossRef]
47. Schneider, A.; Friedl, M.A.; Potere, D. A new map of global urban extent from MODIS satellite data. *Environ. Res. Lett.* **2009**, *4*, 44003. [CrossRef]
48. Waldner, F.; Hansen, M.C.M.C.; Potapov, P.V.P.V.; Löw, F.; Newby, T.; Ferreira, S.; Defourny, P. National-scale cropland mapping based on spectral-temporal features and outdated land cover information. *PLoS ONE* **2017**, *12*, e0181911. [CrossRef] [PubMed]
49. Strahler, A.H.; Boschetti, L.; Foody, G.M.; Friedl, M.A.; Hansen, M.C.; Herold, M.; Mayaux, P.; Morisette, J.T.; Stehman, S.V.; Woodcock, C.E. *Global Land Cover Validation: Recommendations for Evaluation and Accuracy Assessment of Global Land Cover Maps. GOFC-GOLD Report No. 25*; European Communities: Luxembourg, 2006.
50. Herold, M.; Mayaux, P.; Woodcock, C.; Baccini, A.; Schmullius, C. Some challenges in global land cover mapping: An assessment of agreement and accuracy in existing 1 km datasets. *Remote Sens. Environ.* **2008**, *112*, 2538–2556. [CrossRef]
51. Pflugmacher, D.; Krankina, O.N.; Cohen, W.B.; Friedl, M.A.; Sulla-Menashe, D.; Kennedy, R.E.; Nelson, P.; Loboda, T.V.; Kuemmerle, T.; Dyukarev, E.; et al. Comparison and assessment of coarse resolution land cover maps for Northern Eurasia. *Remote Sens. Environ.* **2011**, *115*, 3539–3553. [CrossRef]
52. FAO The Aral Sea Basin. Available online: http://www.fao.org/nr/water/aquastat/basins/aral-sea/index.stm (accessed on 10 January 2018).
53. Cowan, P.J. Geographic usage of the terms Middle Asia and Central Asia. *J. Arid Environ.* **2007**, *69*, 359–363. [CrossRef]

54. Saiko, T.A.; Zonn, I.S. Irrigation expansion and dynamics of desertification in the Circum-Aral region of Central Asia. *Appl. Geogr.* **2000**, *20*, 349–367. [CrossRef]
55. Bekchanov, M.; Ringler, C.; Bhaduri, A.; Jeuland, M. Optimizing irrigation efficiency improvements in the Aral Sea Basin. *Water Resour. Econ.* **2016**, *13*, 30–45. [CrossRef]
56. FAO Aquastat. Available online: http://www.fao.org/nr/water/aquastat (accessed on 10 January 2018).
57. Lal, R.; Suleimenov, M.; Steward, B.A.; Hansen, D.O.; Doraiswamy, P. *Climate Change and Terrestrial Carbon Sequestration in Central Asia*, 1st ed.; Taylor & Francis: Leiden, The Netherlands, 2007.
58. O'Hara, S.L. Irrigation and land degradation: implications for agriculture in Turkmenistan, central Asia. *J. Arid Environ.* **1997**, *37*, 165–179. [CrossRef]
59. Conrad, C.; Lamers, J.P.A.; Ibragimov, N.; Löw, F.; Martius, C. Analysing irrigated crop rotation patterns in arid Uzbekistan by the means of remote sensing: A case study on post-Soviet agricultural land use. *J. Arid Environ.* **2016**, *124*, 150–159. [CrossRef]
60. Levin, V. *Analysis of Agrarian Policy, Management, Agricultural Products, Farming Systems and Income Acquisition Methods in Agriculture of Kyzylorda Region*; Almaty, Kazakhstan, 2010.
61. Kienzler, K. Improving the Nitrogen Use Efficiency and Crop Quality in the Khorezm Region, Uzbekistan. Ph.D. Thesis, Rheinische Friedrich-Wilhelms-Universität Bonn, Bonn, Germany, 2010.
62. FAO Food and Agriculture Organization of the United Nations (FAOSTAT). Available online: http://faostat3.fao.org/faostat-gateway/go/to/home/E (accessed on 10 January 2018).
63. Umirsakov, S.I.; Tautenov, I.A.; Dschamantikov, H.D.; Tochetova, L.A.; Wilhelm, M.A.; Schermagambetov, K.; Baibosinova, S.M.; Abildajeva, S. *Recommendations on Conduction of Spring Field Campaign in Kyzyl-Orda Oblast*; KazAgro Innovazia: Astana, Kazakhstan, 2011. (In Russian)
64. Khalikov, B.; Tillaev, R.S. *Practical Recommendations on Crop Rotations in Uzbekista*; Uzbekistan Cotton Research Institute: Tashkent, Uzbekistan, 2006.
65. Khalikov, B. *New Crop Rotation Systems and Soil Fertility*; Nosirlik Yogdusi Publishing House: Tashkent, Uzbekistan, 2010.
66. Lerman, Z.; Csaki, C.; Feder, G. Agriculture in Transition: Land Policies and Evolving Farm Structures in Post-Soviet Countries; Lexington books, 2004.
67. Didan, K. *MOD13Q1 MODIS/Terra Vegetation Indices 16-Day L3 Global 250m SIN Grid V006*; NASA EOSDIS Land Processes DAAC; NASA: College Park, MD, USA, 2015.
68. Jonsson, P.; Eklundh, L. TIMESAT—A program for analyzing time-series of satellite sensor data. *Comput. Geosci.* **2004**, *30*, 833–845. [CrossRef]
69. Jacquin, A.; Sheeren, D.; Lacombe, J. Vegetation cover degradation assessment in Madagascar savanna based on trend analysis of MODIS NDVI time seriese. *Int. J. Appl. Earth Obs. Geoinf.* **2010**, *12*, 3–10. [CrossRef]
70. Löw, F.; Fliemann, E.; Narvaez Vallejo, A.; Biradar, C. Mapping Agricultural Production in the Fergana Valley Using Satellite Earth Observation—Project Report; Amman, Jordan, 2016.
71. Löw, F.; Waldner, F.; Dubovyk, O.; Akramkhanov, A.; Prishchepov, A.V.; Lamers, J.P.A.; Biradar, C.M. A consolidated data set of cropland abandonment and recultivation for the Aral Sea Basin in Central Asia. *Data* **2018**, in press.
72. Löw, F.; Navratil, P.; Kotte, K.; Schöler, H.F.; Bubenzer, O. Remote sensing based analysis of landscape change in the desiccated seabed of the Aral Sea—A potential tool for assessing the hazard degree of dust and salt storms. *Environ. Monit. Assess.* **2013**, *185*, 8303–8319. [CrossRef] [PubMed]
73. Machwitz, M.; Bloethe, J.; Klein, D.; Conrad, C.; Dech, S. Mapping of large irrigated areas in Central Asia using MODIS time series. In *Proceedings of SPIE 7824, Remote Sensing for Agriculture, Ecosystems, and Hydrology XII, 782403*; SPIE: Toulouse, France, 2010; Volume 49.
74. Clark, M.L.; Aide, T.M.; Grau, H.R.; Riner, G. A scalable approach to mapping annual land cover at 250 m using MODIS time series data: A case study in the Dry Chaco ecoregion of South America. *Remote Sens. Environ.* **2010**, *114*, 2816–2832. [CrossRef]
75. Müller, H.; Rufin, P.; Griffiths, P.; Barros Siqueira, A.J.; Hostert, P. Mining dense Landsat time series for separating cropland and pasture in a heterogeneous Brazilian savanna landscape. *Remote Sens. Environ.* **2015**, *156*, 490–499. [CrossRef]
76. Wolfe, R.E.; Roy, D.P.; Vermote, E. MODIS land data storage, gridding, and compositing methodology: Level 2 grid. *IEEE Trans. Geosci. Remote Sens.* **2002**, *36*, 1324–1338. [CrossRef]

77. Duveiller, G.; Baret, F.; Defourny, P. Crop specific green area index retrieval from MODIS data at regional scale by controlling pixel-target adequacy. *Remote Sens. Environ.* **2011**, *115*, 2686–2701. [CrossRef]
78. Conrad, C.; Schönbrodt-Stitt, S.; Löw, F.; Sorokin, D.; Paeth, H. Cropping intensity in the Aral Sea Basin and its dependency from the runoff formation 2000-2012. *Remote Sens.* **2016**, *8*, 630. [CrossRef]
79. Fischer, G.; Van Velthuizen, H.; Shah, M.; Nachtergaele, F. *Global Agro-Ecological Assessment for Agriculture in the 21st Century: Methodology and Results*; IIASA: Laxenburg, Austria, 2002.
80. IIASA. *FAO Global Agro-Ecological Zones (GAEZ v3.0)*; IIASA: Schloss Laxenburg, Austria, 2012.
81. Breiman, L. Random forests. *Mach. Learn.* **2001**, *45*, 5–32. [CrossRef]
82. Waske, B.; Braun, M. Classifier ensembles for land cover mapping using multitemporal SAR imagery. *ISPRS J. Photogramm. Remote Sens.* **2009**, *64*, 450–457. [CrossRef]
83. Rodriguez-Galiano, V.F.; Ghimire, B.; Rogan, J.; Chica-Olmo, M.; Rigol-Sanchez, J.P. An assessment of the effectiveness of a random forest classifier for land-cover classification. *ISPRS J. Photogramm. Remote Sens.* **2012**, *67*, 93–104. [CrossRef]
84. Rodriguez-Galiano, V.F.; Chica-Olmo, M.; Abarca-Hernandez, F.; Atkinson, P.M.; Jeganathan, C. Random forest classification of Mediterranean land cover using multi-seasonal imagery and multi-seasonal texture. *Remote Sens. Environ.* **2012**, *121*, 93–107. [CrossRef]
85. Mountrakis, G.; Im, J.; Ogole, C. Support vector machines in remote sensing: A review. *ISPRS J. Photogramm. Remote Sens.* **2011**, *66*, 247–259. [CrossRef]
86. Breiman, L.; Friedman, J.; Stone, C.J.; Olshen, R.A. *Classification and Regression Trees*; CRC Press: Boca Raton, FL, USA, 1984.
87. Vapnik, V. *The Nature of Statistical Learning Theory (Statistics for Engineering and Information Science)*, 2nd ed.; Jordan, M., Lauritzen, S.L., Lawless, J.F., Nair, V., Eds.; Springer: Berlin, German, 2000.
88. Mathur, A.; Foody, G.M. Crop classification by support vector machine with intelligently selected training data for an operational application. *Int. J. Remote Sens.* **2008**, *29*, 2227–2240. [CrossRef]
89. Pal, M.; Foody, G.M. Feature selection for classification of hyperspectral data by SVM. *IEEE Trans. Geosci. Remote Sens.* **2010**, *48*, 2297–2307. [CrossRef]
90. Foody, G.M.; Mathur, A. Toward intelligent training of supervised image classifications: directing training data acquisition for SVM classification. *Remote Sens. Environ.* **2004**, *93*, 107–117. [CrossRef]
91. Fauvel, M.; Chanussot, J.; Benediktsson, J.A. Decision fusion for the classification of urban remote sensing images. *IEEE Trans. Geosci. Remote Sens.* **2006**, 2828–2838. [CrossRef]
92. Policar, R. Ensemble based systems in decision making. *IEEE Circuits Syst. Mag.* **2006**, *6*, 21–45. [CrossRef]
93. Waske, B.; van der Linden, S.; Benediktsson, J.A.; Rabe, A.; Hostert, P. Sensitivity of support vector machines to random feature selection in classification of hyperspectral data. *IEEE Trans. Geosci. Remote Sens.* **2010**, *48*, 2880–2889. [CrossRef]
94. Loosvelt, L.; Peters, J.; Skriver, H. Impact of reducing polarimetric SAR input on the uncertainty of crop classifications based on the random forests algorithm. *IEEE Trans. Geosci. Remote Sens.* **2012**, *50*, 4185–4200. [CrossRef]
95. Giacco, F.; Thiel, C.; Pugliese, L.; Scarpetta, S.; Marinaro, M. Uncertainty analysis for the classification of multispectral satellite images using SVMs and SOMs. *IEEE Trans. Geosci. Remote Sens.* **2010**, *48*, 3769–3779. [CrossRef]
96. Löw, F.; Michel, U.; Dech, S.; Conrad, C. Impact of feature selection on the accuracy and spatial uncertainty of per-field crop classification using Support Vector Machines. *ISPRS J. Photogramm. Remote Sens.* **2013**, *85*, 102–119. [CrossRef]
97. Karatzoglou, A.; Meyer, D.; Hornik, K. Support vector machines in R. *J. Stat. Softw.* **2006**, *15*, 1–28. [CrossRef]
98. Congalton, R.G. A review of assessing the accuracy of classifications of remotely sensed data. *Remote Sens. Environ.* **1991**, *37*, 35–46. [CrossRef]
99. Congalton, R.G.; Green, K. *Assessing the Accuracy of Remotely Sensed Data: Principles and Practices*, 2nd ed.; CRC Press Inc.: Boca Raton, FL, USA, 2009; Volume 48.
100. Olofsson, P.; Foody, G.M.; Herold, M.; Stehman, S.V.; Woodcock, C.E.; Wulder, M.A. Good practices for estimating area and assessing accuracy of land change. *Remote Sens. Environ.* **2014**, *148*, 42–57. [CrossRef]
101. Foody, G.M. Classification accuracy comparison: Hypothesis tests and the use of confidence intervals in evaluations of difference, equivalence and non-inferiority. *Remote Sens. Environ.* **2009**, *113*, 1658–1663. [CrossRef]

102. Tayyebi, A.; Pijanowski, B.C.; Linderman, M.; Gratton, C. Comparing three global parametric and local non-parametric models to simulate land use change in diverse areas of the world. *Environ. Model. Softw.* **2014**, *59*, 202–221. [CrossRef]
103. Tayyebi, A.; Pijanowski, B.C. Modeling multiple land use changes using ANN, CART and MARS: Comparing tradeoffs in goodness of fit and explanatory power of data mining tools. *Int. J. Appl. Earth Obs. Geoinf.* **2014**, *28*, 102–116. [CrossRef]
104. Fawcett, T. An introduction to ROC analysis. *Pattern Recognit. Lett.* **2006**, *27*, 861–874. [CrossRef]
105. Olofsson, P.; Foody, G.M.; Stehman, S.V.; Woodcock, C.E. Making better use of accuracy data in land change studies: Estimating accuracy and area and quantifying uncertainty using stratified estimation. *Remote Sens. Environ.* **2013**, *129*, 122–131. [CrossRef]
106. Card, D. Using know map category marginal frequencies to improve estimates of thematic map accuracy. *Photogramm. Eng. Remote Sens.* **1982**, *48*, 432–439.
107. Stehman, S.V. Estimating the Kappa coefficient and its variance under stratified random sampling. *Photogramm. Eng. Remote Sens.* **1996**, *62*, 401–407.
108. Moran, P.A.P. Notes on continuous stochastic phenomena. *Biometrika* **1950**, *37*, 17–23. [CrossRef] [PubMed]
109. Anselin, L. Local indicators of spatial association—LISA. *Geogr. Anal.* **1995**, *27*, 93–115. [CrossRef]
110. Lambert, M.-J.; Waldner, F.; Defourny, P. Cropland Mapping over Sahelian and Sudanian Agrosystems: A Knowledge-Based Approach Using PROBA-V Time Series at 100-m. *Remote Sens.* **2016**, *8*, 232. [CrossRef]
111. Colditz, R.R.; López Saldaña, G.; Maeda, P.; Espinoza, J.A.; Tovar, C.M.; Hernández, A.V.; Benítez, C.Z.; Cruz López, I.; Ressl, R. Generation and analysis of the 2005 land cover map for Mexico using 250m MODIS data. *Remote Sens. Environ.* **2012**, *123*, 541–552. [CrossRef]
112. Prishchepov, A.V.; Müller, D.; Butsic, V.; Radeloff, V.C. Sensitivity of Spatially Explicit Land-Use Logistic Regression Models to the Errors Land-Use Change Maps. Ph.D. Thesis, International Environmental Modelling and Software Society (iEMSs), Leipzig, Germany, 2012.
113. Huang, C.; Davis, L.S.; Townshend, J.R.G. An assessment of support vector machines for land cover classification. *Int. J. Remote Sens.* **2002**, *23*, 725–749. [CrossRef]
114. Waldner, F.; Jacques, D.C.; Löw, F. The impact of training class proportions on binary cropland classification. *Remote Sens. Lett.* **2017**, *8*, 1123–1132. [CrossRef]
115. Müller, D.; Leitão, P.J.; Sikor, T. Comparing the determinants of cropland abandonment in Albania and Romania using boosted regression trees. *Agric. Syst.* **2013**, *117*, 66–77. [CrossRef]
116. Smaliychuk, A.; Müller, D.; Prishchepov, A.V.; Levers, C.; Kruhlov, I.; Kuemmerle, T. Recultivation of abandoned agricultural lands in Ukraine: Patterns and drivers. *Glob. Environ. Chang.* **2016**, *38*, 70–81. [CrossRef]
117. Waldner, F.; De Abelleyra, D.; Verón, S.R.; Zhang, M.; Wu, B.; Plotnikov, D.; Bartalev, S.; Lavreniuk, M.; Skakun, S.; Kussul, N.; et al. Towards a set of agrosystem-specific cropland mapping methods to address the global cropland diversity. *Int. J. Remote Sens.* **2016**, *37*, 3196–3231. [CrossRef]
118. *FAO-UNESCO Irrigation in Central Asia in Figures—AQUASTAT Survey 2012*; FAO: Rome, Italy, 2013; p. 246.
119. Prishchepov, A.V.; Radeloff, V.C.; Baumann, M.; Kuemmerle, T.; Müller, D. Effects of institutional changes on land use: Agricultural land abandonment during the transition from state-command to market-driven economies in post-Soviet Eastern Europe. *Environ. Res. Lett.* **2012**, *7*, 24021. [CrossRef]
120. Kuemmerle, T.; Hostert, P.; Radeloff, V.C.; Linden, S.; Perzanowski, K.; Kruhlov, I. Cross-border Comparison of Post-socialist Farmland Abandonment in the Carpathians. *Ecosystems* **2008**, *11*, 614–628. [CrossRef]
121. Nurbekov, A. *Sustainable Agricultural Practices in the Drought Affected Region of Karakalpakstan (Phase II)*; Final Report of FAO/TCP/3102 (A); FAO: Tashkent, Uzbekistan, 2007.
122. Robinett, D.; Miller, D.; Bedunah, D. Central Afghanistan Rangelands. *Soc. Range Manag.* **2008**, *30*, 2–12. [CrossRef]
123. Anderson, K.; Swinnen, J. *Distortions to Agricultural Incentives in Europe´s Transition Economies*; Anderson, K., Swinnen, J., Eds.; The World Bank: Washington, DC, USA, 2008.
124. Lerman, Z. Land reform, farm structure, and agricultural performance in CIS countries. *China Econ. Rev.* **2009**, *20*, 316–326. [CrossRef]